WARWICK
THE UNIVERSITY OF WARWICK

**Manuscript version: Author's Accepted Manuscript**
The version presented in WRAP is the author's accepted manuscript and may differ from the published version or Version of Record.

**Persistent WRAP URL:**
http://wrap.warwick.ac.uk/158141

**How to cite:**
Please refer to published version for the most recent bibliographic citation information.

**Copyright and reuse:**
The Warwick Research Archive Portal (WRAP) makes this work by researchers of the University of Warwick available open access under the following conditions.

Copyright © and all moral rights to the version of the paper presented here belong to the individual author(s) and/or other copyright owners. To the extent reasonable and practicable the material made available in WRAP has been checked for eligibility before being made available.

Copies of full items can be used for personal research or study, educational, or not-for-profit purposes without prior permission or charge. Provided that the authors, title and full bibliographic details are credited, a hyperlink and/or URL is given for the original metadata page and the content is not changed in any way.

**Publisher's statement:**
Please refer to the repository item page, publisher's statement section, for further information.

For more information, please contact the WRAP Team at: wrap@warwick.ac.uk.

**warwick.ac.uk/lib-publications**

# Clathrin- The Molecular Shape Shifter

Katherine M. Wood[1] and Corinne J. Smith[2].

[1]Warwick medical school, University of Warwick, Coventry, U.K.; [2]School of life sciences, University of Warwick, Coventry, U.K.

Correspondence: Corinne J. Smith (corinne.smith@warwick.ac.uk)

## Abstract

Clathrin is best known for its contribution to clathrin-mediated endocytosis yet it also participates to a diverse range of cellular functions. Key to this is clathrin's ability to assemble into polyhedral lattices that include curved football or basket shapes, flat lattices or even tubular structures. In this review we discuss clathrin structure and coated vesicle formation, how clathrin is utilised within different cellular processes including synaptic vesicle recycling, hormone desensitisation, spermiogenesis, cell migration and mitosis, and how clathrin's remarkable 'shapeshifting' ability to form diverse lattice structures might contribute to its multiple cellular functions.

## Introduction

Eukaryotic cells use endocytosis to internalise cargo from their extracellular environment, in which invagination of the plasma membrane creates a vesicle or tubule that is cleaved off and released into the cytoplasm of the cell (1–4). In receptor mediated endocytosis (RME) receptors on cell surfaces target specific cargo for import, which when internalised is transported to endosomes. The cargo may then be recycled back to the cell membrane,

transported intracellularly or delivered to lysosomes for degradation (5–7). Clathrin mediated endocytosis (CME) is the most studied form of RME and is believed to be the major endocytic process in cells (8). CME was first discovered in 1964 and is named after the clathrin coated vesicles (CCV) of around 60 nm to 135 nm in diameter that form from cell membranes in order to achieve this. The clathrin coat is formed from the scaffold protein clathrin and other CME adaptor proteins (9–13). Clathrin is highly evolutionarily conserved within eukaryotes and is involved in multiple cellular processes including mitosis, spermiogenesis, hormone desensitisation, cell migration, synaptic vesicle (SV) recycling, and intracellular trafficking (14–19). Figure 1 illustrates the processes in which clathrin is involved. Defects within CME are associated with several pathological conditions, including Parkinson's disease, Alzheimer's disease, HIV/AIDs, and autosomal recessive hypercholesterolemia (20–27).

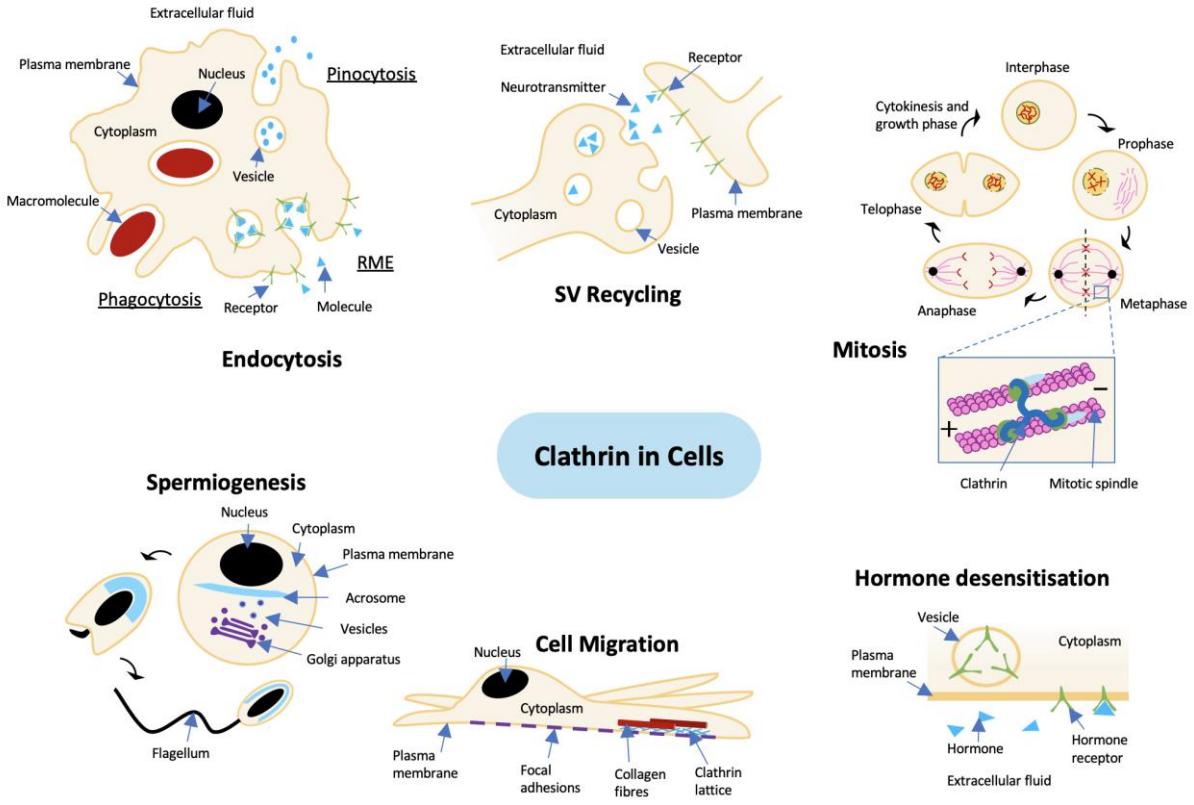


**Figure 1 – Clathrin-mediated endocytosis in cellular processes**

**Schematic diagram demonstrating the variety of cellular processes in which clathrin is used, including but not limited to endocytosis, spermiogenesis, cell migration, hormone desensitisation, mitosis, and SV recycling (1–4,14–19). Diagram is not to scale.**

For CME to occur clathrin is required to form a coat bound to the cell membrane, but clathrin cannot directly interact with cell membrane lipids and proteins and thus relies on CME adaptor proteins to form these connections (20,28). Once a clathrin coat starts to form, invagination can begin, as the formation of the clathrin coat and the presence of CME adaptors such as BAR-domain proteins and epsin alter the balance of forces stabilising the cell membrane to allow membrane bending to occur (1,29–31). For invagination to occur, the CME adaptors need to contribute forces of the order of picoNewtons so that factors that make bending the membrane challenging, such as high membrane tension, internal hydrostatic pressure, and cargo properties, can be overcome (1,11,32,33). These picoNewton forces could be provided via the consequences of actin polymerisation and crosslinking, involving hydrolysis of ATP, interactions of BAR domain proteins with the membrane and one another, molecular crowding or clathrin assembly (34). Despite our understanding of the challenges of membrane invagination, there is still ongoing debate regarding how clathrin coats assemble, the role and nature of clathrin lattice rearrangement, how CME adaptors interact and cooperate to produce CCVs and clathrin coated pits (CCP), and how the CME process is regulated to ensure the successful formation of vesicles saturated with cargo. In this review, we will discuss current knowledge of clathrin structure and how this contributes to the molecular mechanism of CME, how clathrin is utilised during different cellular processes, and how clathrin's remarkable 'shapeshifting' ability to form diverse lattice structures might contribute to its multiple cellular functions.

57 ## Clathrin structure

58 Clathrin forms a three-legged structure called a triskelion composed of three clathrin heavy
59 chains (CHC) ~190 kDa in size, and three clathrin light chains (CLC) ~25 kDa in size (35,36). CHC
60 consists of five domains called the trimerization domain, proximal domain, distal domain,
61 ankle domain, and terminal domain, as shown in figure 2A (37). The trimerization domain
62 consists of a 45-residue carboxy-terminal segment responsible for binding to other CHC
63 carboxy terminal regions to create a protein complex in the form of a triskelion structure. The
64 next region consists of 42 zig-zagging alpha-helices that form the proximal, distal and ankle
65 domains, which are responsible for the curved legs of the clathrin triskelion that create its
66 tripod-like structure. The final region, the terminal domain, consists of a seven-bladed WD40
67 repeat beta-propeller at the amino-terminal responsible for interactions between clathrin
68 and other CME adaptor proteins. The structure of a CLC consists of a long alpha-helix in the
69 centre of its structure responsible for interactions with the CHC proximal domain, disordered
70 terminal regions whose interaction with CHC is unclear, and a folded helical region close to
71 the C terminus that is embedded in and stabilises the CHC trimerization domain (37–40). The
72 structure of a bovine clathrin triskelion and the location of CLCs, CHCs and CHC domains is
73 shown in figure 2B.

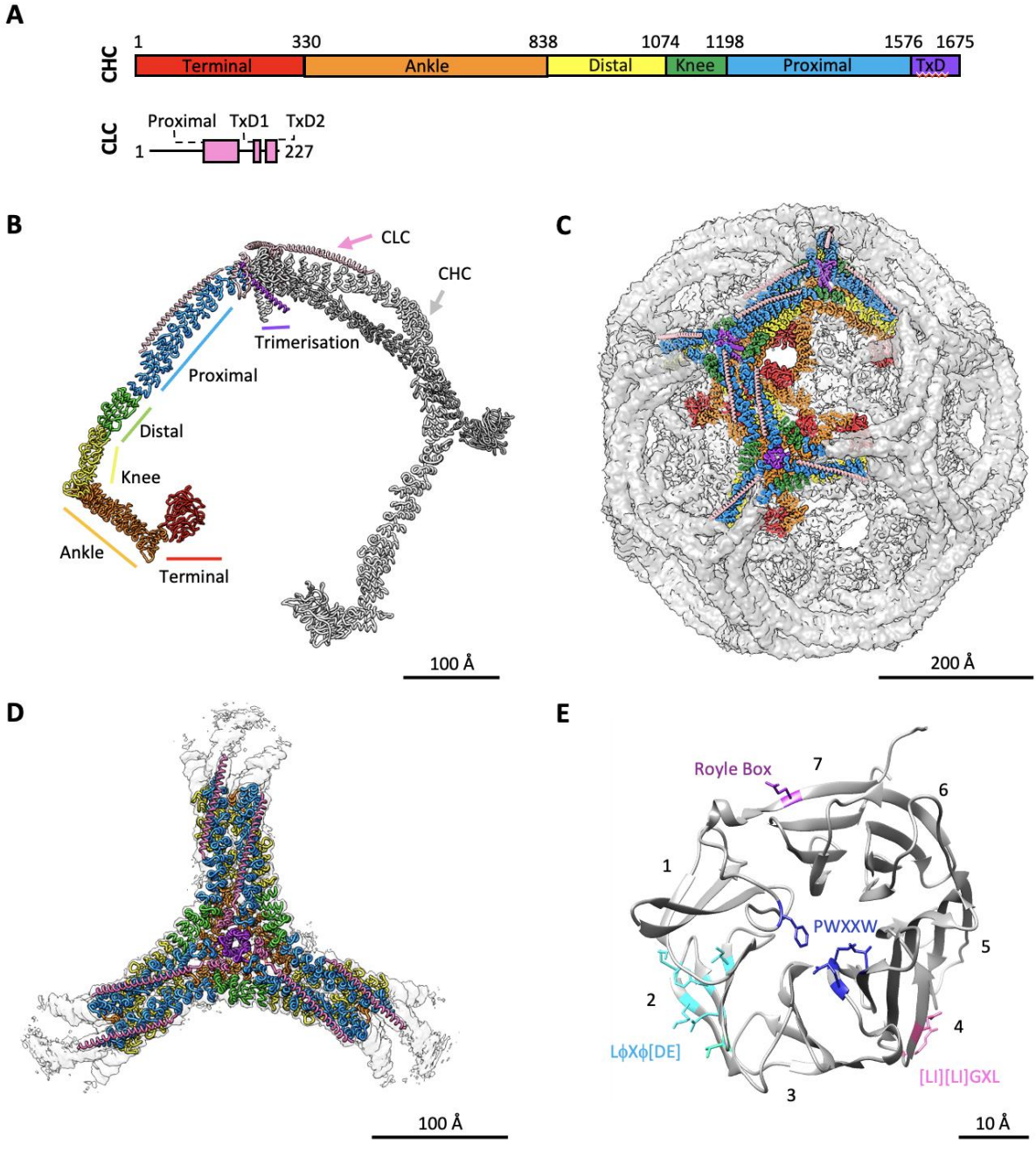


**Figure 2 – Clathrin structure**

**A) Domain organisation within CLC and CHC (41). B) Model of a clathrin triskelion including the bovine CHC model (Protein Data Bank (PDB): 3IYV) (37) informed by fitting the high resolution x-ray structure (PDB: 1B89) (42) into cryo-EM density maps and the porcine CLC model produced from cryo-EM density maps (PDB: 6SCT) (41). C) Model of a bovine clathrin cage (EMD: 5119) with fitted clathrin triskelion model produced from cryo-EM density maps (PDB: 1XI5) (37). D) Recent 4.7 Å porcine clathrin hub structure with fitted PDB model (PDB: 6SCT) produced from cryo-EM density maps (EMD: 0126) (41). E) Model of a rat CHC terminal domain produced from x-ray diffraction density (PDB: 1BPO), with location of binding sites for different motifs highlighted (43). All structure visualization was performed with UCSF Chimera (44).**

Clathrin triskelia interact with each other to form clathrin cages *in vitro*, and clathrin lattices, CCPs and CCVs *in vivo*. The size and shape of clathrin coats and lattices varies and this allows

86 vesicles to accommodate the required size and quantity of cargo being imported. For
87 example, bovine brain CCVs have smaller diameters of 60 - 80 nm compared to human
88 placenta CCVs that produce larger CCVs of 100 – 135 nm (10,45,46). This size variability is
89 possible due to clathrin's ability to assemble into different configurations, including
90 pentagon and hexagon arrangements, and, less frequently, heptagons and squares (10,41).
91 Clathrin assembles into empty coat structures *in vitro*, also known as clathrin cages or
92 baskets, if placed in a buffer at pH 6.5 or less with magnesium and calcium ions present (35).
93 Formation of clathrin cages *in vitro* has allowed cryo-electron microscopy analysis of these
94 large multi-protein complexes at high resolution, which led to the production of the 7.8 Å D6
95 dihedral symmetry clathrin coat structure shown in figure 2C, and the more recent 4.7 Å
96 clathrin consensus hub substructure demonstrated in figure 2D (37,41,47,48). Within each of
97 these structures, a clathrin triskelion is centred at each hub or lattice point, with the triskelion
98 legs interacting with other triskelia which causes the legs to bend inwards. The degree of
99 bending of the triskelion leg varies depending upon the clathrin cage or lattice configuration,
100 indicating some flexibility most likely due to the arrangement of paired alpha-helices oriented
101 perpendicular to the long leg axis in the proximal, distal and ankle domains, which would be
102 able to change conformation to produce a variety of different leg configurations (37,41).

## 103 The clathrin terminal domain

104 The clathrin terminal domain is the primary interaction point between clathrin and CME
105 adaptors. It consists of a seven-bladed β-propeller at the CHC amino-terminal joined to short
106 α-helices that connect to the ankle region of the CHC. X-ray crystallography has been used to
107 determine the terminal domain's structure to 2.6 Å, shown in figure 2E (43). Additional
108 analysis of terminal domain interactions with CME adaptors has identified four binding sites

109 within the seven-bladed β-propeller called the clathrin box, the W-box, the arrestin box and
110 the Royle box, indicated in figure 2E (20). The clathrin box is located in a groove between
111 blades one and two of the β-propeller and binds to the highly conserved clathrin box motif
112 which comprises acidic and bulky hydrophobic residues L(L, I)(D, E, N)(L, F)(D, E) (LϕXϕ[DE])
113 (49). The clathrin box motif has been found in several adaptors including the β3-appendage
114 of AP3, amphiphysin, arrestin3 segments, and β-arrestin 1 and β-arrestin 2 (50–54). The
115 arrestin box is located between blades four and five of the β-propeller and binds to the
116 arrestin box motif, which is found in arrestin proteins and consists of residues [LI][LI]GXL (55).
117 The W-box is located towards the centre of the β-propeller rather than on the blades'
118 outskirts like the other binding sites and binds to the W-box motif, which consists of residues
119 PWXXW. Amphiphysin 1 is one CME adaptor that contains a W-box motif which binds to the
120 W-box with a compact helical structure as determined at 2.3 Å via x-ray crystallography (56).
121 The final binding site, called the Royle box, is found on the seventh blade of the β-propeller.
122 The nature of the motif required to bind to the Royle box is currently unknown (57) but
123 Muenzner et al 2017 present crystal structures showing three different peptides bound to the
124 Royle box which facilitated further definition of this site (58). This study together with work
125 from Zhou et al 2015 (59) also suggests there is a degree of degeneracy in the sequence of
126 motifs interacting with different terminal domain sites, enabling some motifs to bind to more
127 than one site on the clathrin terminal domain.

128 Other motifs, called DLL and DLF motifs that have been identified in a number of clathrin
129 adaptors including assembly protein 180 kDa (AP180), which can also bind to the clathrin
130 terminal domain via weak interactions with a Kd value of around 2 x $10^{-4}$ M (60,61). Since
131 there are multiple such motifs within the AP180 sequence their combined effect, or avidity,

132 produces stable interactions (61). As individual DLL and DLF motifs only associate with clathrin
133 via weak interactions, this allows for rapid association and dissociation between CME
134 adaptors and clathrin, which could be vital for AP180 to capture clathrin whilst allowing a
135 clathrin lattice to form (20,62).

## 136 Clathrin mediated endocytosis

137 CME involves the coordination of around fifty different adaptor or accessory proteins, which
138 can interact with clathrin and or each other to complete different stages of CME. Each adaptor
139 has a different role and may be involved in one or several stages, which have so far been
140 described as nucleation and assembly, stabilisation and maturation, neck constriction and
141 scission, and clathrin uncoating (11,63,64). A visual representation of each CME stage is
142 presented in figure 3. During CME, adaptor proteins may arrive at CME sites in stages,
143 resulting in fluctuations of local concentrations of adaptor proteins depending on the stage
144 clathrin assembly has reached (63,65–68).

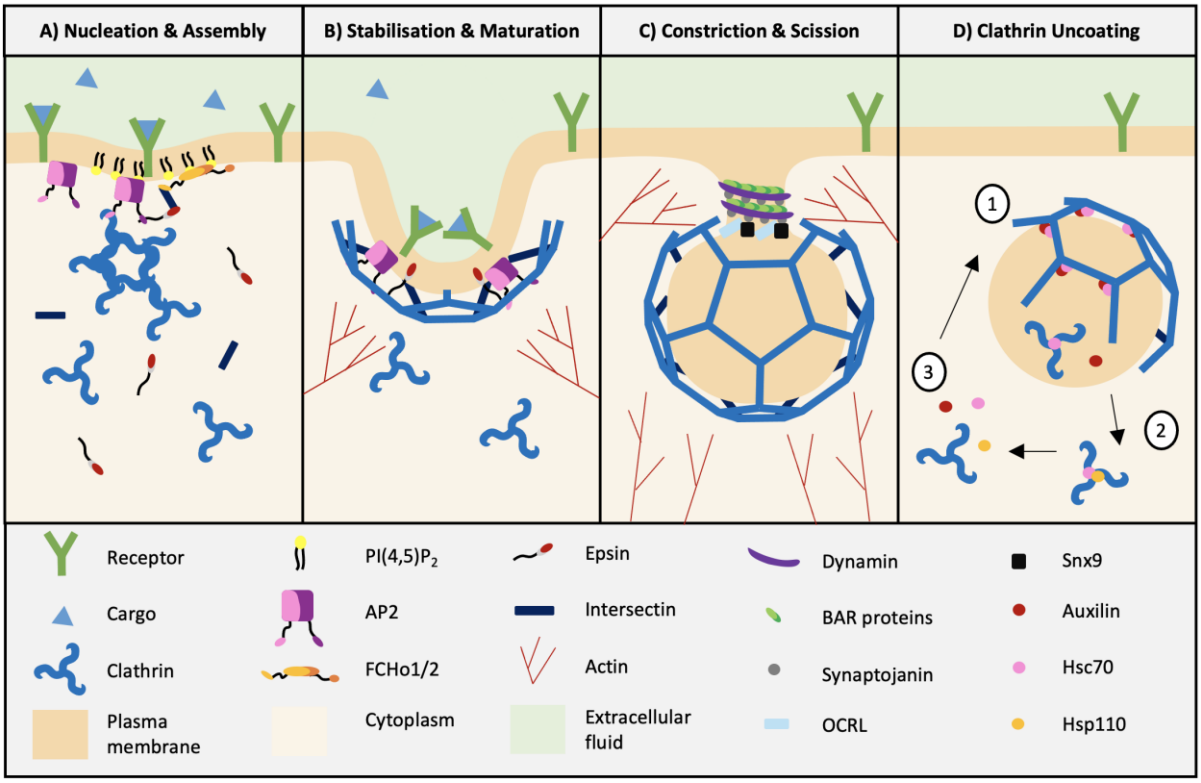


**Figure 3 – Stages in clathrin mediated endocytosis**

**Schematic diagram illustrating different stages in CME, including A) nucleation and assembly, followed by B) stabilisation and maturation, followed by C) constriction and scission, followed by D) clathrin uncoating. Figure is not to scale.**

## Nucleation and assembly

Initiation of CME occurs upon formation of an 'interaction nucleus', which is required for recruiting adaptors and forming a clathrin coat. How this nucleus develops is under debate, as it could be due to interactions between multiple accessory proteins including Fer/Cip4 homology domain-only proteins 1 and 2 (FCHo1/2), adaptor protein 2 (AP2), epidermal growth factor receptor substrate 15 (Eps15), Eps15 receptor (Eps15R), intersectins 1/2, and potentially other adaptors that have yet to be identified (29,66,69). However, evidence from several groups indicates that the FCHo1/2 complex and the AP2 complex could be the primary initiators for the formation of the CME nucleus (29,69–73). Once the CME nucleus has formed, adaptor proteins can recruit cargo to the site through interactions with the cytosolic regions

160 of transmembrane cargo or transmembrane cargo receptors, allowing the importing of cargo
161 and associated lipids into the cell (74–77). Some of the known cargo adaptors include AP2,
162 FCHo1, Eps15, and clathrin-assembly lymphoid myeloid leukaemia protein (CALM) (78,79). As
163 these four adaptors are associated with initiation, it seems possible that cargo can play a role
164 in recruiting adaptor proteins to form a nucleation point and thereby initiate CME (80–82).

165 Despite the large surface area of cell membranes, CME nucleation tends to occur at spatially
166 distinct sites, for example as in neuronal synapses (83). The location of CME nucleation may
167 be due to differing levels of availability of CME adaptors across the cell, such as AP2 and
168 phosphatidylinositol 4,5-bisphosphate (PI(4,5)$P_2$), and the local formation of cortical actin
169 (84). PI(4,5)$P_2$ is necessary for nucleation site formation since depletion of PI(4,5)$P_2$ prevents
170 the formation of CCPs , and many CME adaptors bind to PI(4,5)$P_2$ at the cell membrane
171 (85,86). It is possible that different local concentrations of PI(4,5)$P_2$ and CME adaptors may
172 explain why CME occurs at spatially distinct sites (85,86). Nucleation can occur randomly at
173 positions in the cell membrane where endocytosis does not usually occur, possibly due to
174 stochastic collisions between CME adaptors, however, the majority of nucleation sites are
175 formed at spatially distinct locations (70,76).

176 For CME to occur at spatially distinct sites, there must be some level of organisation,
177 potentially through the use of nucleation factors and organisers such as FCHo1/2 and Sorting
178 Nexin 9 (SNX9), for example. Changes in the expression levels of FCHo1/2 and SNX9 have been
179 found to impact the quantity of CCP formation and spatial clustering of CCPs, respectively
180 (29,84). FCHo1/2 is responsible for engaging with AP2 and the scaffold proteins eps15 and
181 intersectin to sculpt the nucleation site to create a CCP, and so by having high local
182 concentrations of FCHo1/2, cells can ensure high quantities of CCPs are formed which is of

183 great functional value for, for example, neuron synapses which require localised synaptic
184 vesicle recycling (29,70).

185 Quality control in CME is critical to ensure that productive vesicles are developed that contain
186 sufficient cargo. CCP intermediates are frequently aborted, as observations of nucleation
187 events have shown weak or short-lived CCPs in cells, but multiple checkpoints may determine
188 the level of CME turnover (76). Checkpoints may include the presence or quantity of cargo in
189 CCPs, the ubiquitination of cargo adaptors, or other factors (4,76,82,87,88). If CCPs are
190 incapable of clearing the checkpoint, then CCP formation can be delayed or aborted. The
191 recruitment of dynamin could also be viewed as a checkpoint controlling the level of CME
192 turnover, as dynamin is responsible for the final stage of CME, scission (89).

193 ## Stabilisation and maturation

194 Once a CCP has formed, the CCP undergoes stabilisation and maturation so that it develops a
195 vesicle-like structure filled with cargo. Several proteins that have either direct roles in
196 membrane bending or act indirectly by influencing clathrin assembly are recruited to the CCP,
197 including epsin, CALM, clathrin, heat shock cognate 71 kDa protein (Hsc70), Cyclin G-
198 associated kinase (GAK), auxilin and actin. Clathrin's ability to form lattices and polyhedral
199 cages consisting predominantly of hexagonal and pentagonal arrangements helps stabilise
200 and potentially induce curvature in cell membranes (10,41). When bound to clathrin, the
201 amphipathic helices found within epsin and CALM can wedge into the cell membrane to bend
202 and curve the membrane in the area (13,90,91). CLCs help to stabilise the developed
203 membrane curvature by binding to CHCs in clathrin lattices which causes clathrin lattices to
204 become more rigid (92,93). Hsc70, GAK and auxilin, the adaptors responsible for clathrin

205 uncoating, have also been proposed to be involved in reorganising the clathrin lattice as the
206 CCP develops (94–99).

207 The actin cytoskeleton helps to further stabilise the CCP by assembling around CCP sites,
208 particularly around clathrin coats and the base of CCPs, potentially acting as a scaffold that
209 can generate and transmit a force to promote membrane curvature (100–103). The
210 presence of the actin cytoskeleton helps support CME during periods of high membrane
211 tension, as live cell imaging studies have shown that perturbations in the actin cytoskeleton
212 inhibit CME (65,83,104–110). For actin to stabilise or contribute to membrane bending it
213 needs to couple with the clathrin coat. This is thought to occur via epsin and (Huntington-
214 interacting protein 1-related protein) HIP1R, both of which are known to bind to actin,
215 clathrin and PI(4,5)$P_2$ (111–115).

## 216 Neck constriction and scission

217 Once the CCP has fully formed, Bin/Amphiphysin/Rvs (BAR) domain proteins will bind to the
218 CCP and, when recruited in high densities, will tubulate the membrane to constrict the CCP
219 neck (116–118). The level of membrane curvature has been shown to influence recruitment
220 of BAR domain proteins, with F-BAR domain and N-BAR domain proteins being preferentially
221 recruited to low and high membrane curvature respectively (119,120). Once the neck of the
222 CCP has constricted, and the vesicle is ready to be released into the cell, BAR domain proteins
223 will recruit the GTPase dynamin to conduct the scission process (119,121,122). Dynamin
224 assembles around the neck of the vesicle as tight oligomers around 20 nm in diameter, and
225 upon GTP binding and hydrolysis, constrict to stimulate membrane fission (123). However, it
226 should be noted that scission cannot occur by dynamin constriction alone, as the scission

227 process requires the presence of several dynamin partners to ensure that preconditions for
228 scission are met, such as control of membrane tension and/or remodelling by actin,
229 synaptojanin and endophilin (124–128). How the scission process occurs in vivo is thus still
230 under debate.

## 231 Clathrin uncoating

232 Upon the CCV being released from the membrane and into the cell, the clathrin coat is
233 disassembled. Removal of the clathrin coat allows the vesicle to be trafficked to the early
234 endosome and CME adaptors associated with the clathrin coat to be recycled. Synaptojanin
235 and Oculocerebrorenal syndrome of Lowe inositol polyphosphate 5-phosphatase (OCRL1)
236 have been implicated in the uncoating of clathrin-coated vesicles and have been proposed to
237 act via dephosphorylation of PI(4,5)$P_2$ to PI(4)P (24,129–134). Loss of PI(4,5)$P_2$ from the CCV
238 is thought to weaken binding of coated vesicle adaptors such as AP-2, AP180 and epsin (134–
239 136), and has been proposed to stimulate recruitment of the chaperone auxilin (94,137–141),
240 which in turn recruits the ATPase Hsc70 and adenosine triphosphate (ATP) via its J-domain to
241 enable clathrin disassembly (95,142). The phosphatase and tensin homolog deleted on
242 chromosome ten (PTEN) domain within auxilin is important for auxilin to bind to the CCV
243 membrane, via interactions with negatively charged lipids such as PI(4,5)$P_2$ (132,133,143).
244 The PTEN domain is not essential for clathrin uncoating but does increase auxilin's functional
245 efficiency, potentially by allowing auxilin to be positioned in a suitable orientation for
246 efficient clathrin uncoating (140,143–145). The J-domain in auxilin, however, is vital for
247 clathrin coat disassembly due to its role in recruiting Hsc70 bound to ATP to assembled
248 clathrin. Auxilin has been shown to act catalytically, enabling recruitment of multiple Hsc70
249 molecules to CCVs for clathrin disassembly. (139,146–149).

250 The binding of Hsc70 to auxilin's J-domain occurs predominantly via electrostatic interactions,
251 with auxilin surface residues Tyr866, Arg867, Lys868, His874, Asp876 and Lys877 being
252 involved in crucial electrostatic interactions with Hsc70 (150,151). Upon recruitment to a CCV,
253 the Hsc70-ATP complex binds to the QLMLT motif at the CHC carboxy-terminus. The three
254 copies of the QLMLT motif available per triskelion provide Hsc70 with the opportunity to bind
255 to up to three sites per clathrin vertex (141,147,152–154). *In vitro* studies of have shown that,
256 when bound to auxilin and clathrin, the ATPase activity of Hsc70 is enhanced, which in cells
257 would likely promote vesicle uncoating (148). Upon ATP hydrolysis, Hsc70 binds stably to
258 clathrin, and the J-domain is released, setting in train events leading to clathrin disassembly
259 (153,155,156). The stability of the clathrin coat will impact the level of structural perturbation
260 required to break triskelion interactions and thus will impact the rate of uncoating and the
261 number of Hsc70 molecules required for coat disassembly (155). As few as one Hsc70
262 molecule for every two clathrin trimers has been observed for initiating clathrin coat
263 disassembly, but this stoichiometric value depends on pH (154,155,157). CLCs help regulate
264 the interaction between auxilin and clathrin to control clathrin coat stabilisation and control
265 auxilins ability to perform catalytically (147). Regulation of auxilin is achieved via
266 phosphorylation of CLCs which promote auxilin dissociation from clathrin (147,158).

267 As clathrin coats are disassembled, triskelia have been observed in yeast to separate from the
268 CCV as partially uncoated intermediates consisting of two or more triskelia which will
269 continue to depolymerise in the cytosol (159). The depolymerised clathrin triskelia remain
270 bound to Hsc70 and adenosine diphosphate (ADP), but auxilin dissociates (140). *In vitro*
271 experiments show that Hsc70 and ADP remain bound to dissociated triskelia, leading the
272 clathrin coat disassembly reaction to follow burst kinetics, where the addition of a limited

273 quantity of Hsc70 causes an initial burst of rapid uncoating followed by a slower steady-state
274 rate where most of the Hsc70 remains bound to the dissociated triskelia (148,154,160). The
275 Hsc70-ADP complex can be released from clathrin by the nucleotide exchange factor heat
276 shock protein 110 (Hsp110) which allows ADP to dissociate from Hsc70 and ATP to bind, thus
277 allowing Hsc70 and clathrin to be recycled for additional rounds of endocytosis (161–165).

278 *In vitro* studies of clathrin cage disassembly have shown that a ratio of one auxilin molecule
279 per clathrin triskelion is sufficient for clathrin to disassemble at the maximum rate, although
280 up to three auxilins can be bound per vertex in cages (160). In cells, auxilin appears to bind to
281 CCVs in transient bursts immediately after scission of CCPs occurs, with only a small number
282 of auxilin molecules observed, ranging from 2 to 20, bound to CCVs of 36 and 100 clathrin
283 trimers in size (94,132,166). However, both in cells and in *in vitro* studies, auxilin has been
284 shown to act catalytically, with one auxilin molecule capable of recruiting multiple Hsc70
285 molecules in sequential order and potentially moving to different clathrin vertices upon
286 dissociation from clathrin after ATP hydrolysis (132,154,160). While maximal rates of
287 disassembly *in vitro* have been shown to require Hsc70 to be present in excess compared with
288 clathrin and auxilin (160), the situation in cells is different. It has been inferred from studies
289 in a human cell line that CCVs formed of around 60 clathrin trimers have less than 10 Hsc70
290 molecules bound at a time during uncoating (132). This difference could be due to the
291 presence of nucleotide exchange factors in cells that would facilitate recycling of Hsc70 and
292 to the possibility that disassembly at the maximum rate is not utilised under cellular
293 conditions.

294 The mechanics by which Hsc70 and auxilin disassemble clathrin coats is intriguing because of
295 the intricate shape of clathrin assemblies and the comparatively small size of the Hsc70 and

296 auxilin molecules that achieve disassembly. Discussion has so far centred around two main
297 models: the steric wedge/Brownian ratchet model, and the entropic pulling or wrecking ball
298 model. A schematic representation of each model is presented in figure 4. The steric wedge
299 model proposes that when auxilin recruits Hsc70, this results in an increase in the excluded
300 volume below the clathrin coat vertices that stabilises a locally strained conformation.
301 Disassembly is favoured by an accumulation of these distortions caused as further Hsc70
302 molecules bind favours disassembly (141,153).

303 Following ATP hydrolysis, Hsc70 no longer binds to the auxilin J domain and becomes tightly
304 associated with the flexible clathrin carboxy-terminal domain, with the potential to move
305 freely, as if a ball on a string, unless sterically hindered by the surrounding structures of the
306 clathrin vertex. The entropic pulling model suggests that the increase in entropy occasioned
307 by increased freedom of movement when Hsc70 moves away from the constraints of the
308 clathrin vertex creates a directional force that pulls on the clathrin carboxy-terminal domain
309 and ultimately disrupts clathrin proximal-distal interactions (99,167–169).

310 By showing that attachment of Fab fragments bound to clathrin at the Hsc70 binding site
311 could cause cage disassembly, Sousa et al 2019 (167) elegantly demonstrated that the energy
312 of ATP hydrolysis was not required to disassemble clathrin per se. When the Fab fragment
313 binding site was moved away from the clathrin vertex, clathrin disassembly continued,
314 suggesting that physical leverage of Hsc70 against the clathrin vertex was not critical for
315 clathrin disassembly. However, disassembly became progressively slower as the distance of
316 the Fab/Hsc70 binding site from the clathrin vertex was increased and was consistent with
317 the effect on rate predicted by the calculations of De los Rios and Goloubinoff, lending weight

318 to the proposal that the driving force for disassembly lay with an entropic pulling/collision

319 pressure model (168).

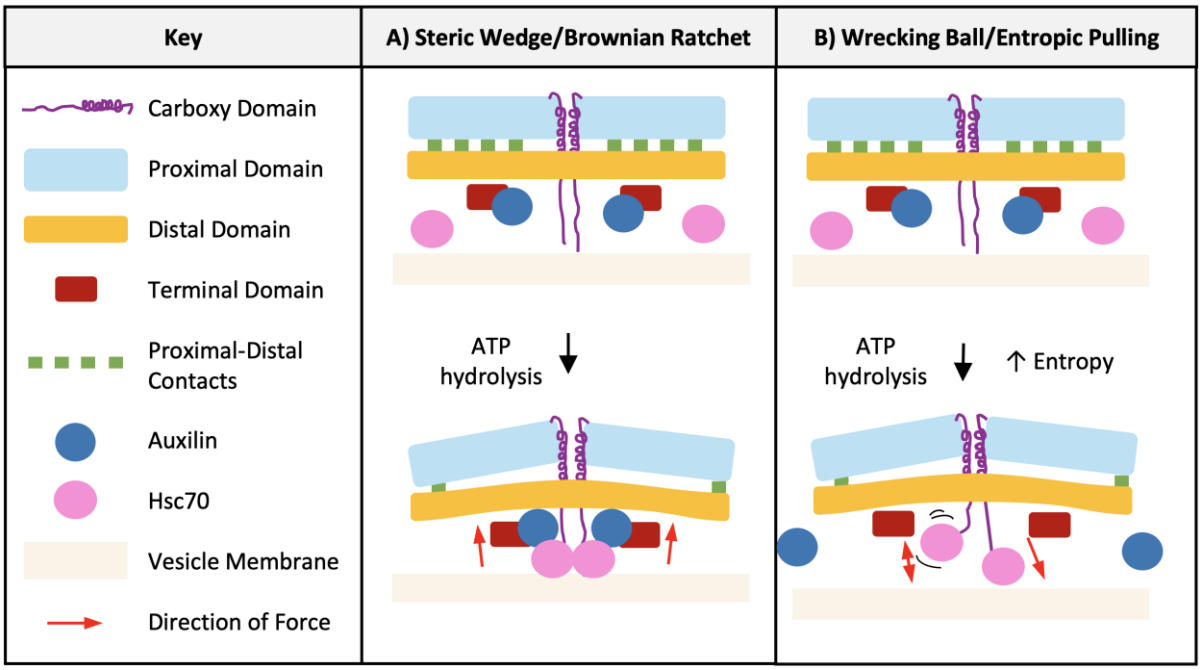


320

321 **Figure 4 – Models for clathrin cage disassembly**

322 **Schematic diagram demonstrating two different models for hsc70 driven disassembly of clathrin cages,**
323 **including A) the steric wedge/Brownian ratchet model, and B) the wrecking ball/entropic pulling model.**
324 **Diagram is not to scale.**

## 325 Diversity of clathrin function in cells

326 The import of molecules into cells via clathrin-mediated endocytosis has been well-studied

327 over many years and comprehensively reviewed (20,170,171). However, clathrin plays more

328 diverse cellular roles that go beyond internalisation of cargo. Here we discuss the diversity of

329 roles CME, and elements of CME machinery, in synaptic vesicle recycling, hormone

330 desensitisation and spermiogenesis, and how clathrin participates in creating other

331 structures, such as tubules and bridges, to aid with cellular migration and mitosis (See Figure

332 5).

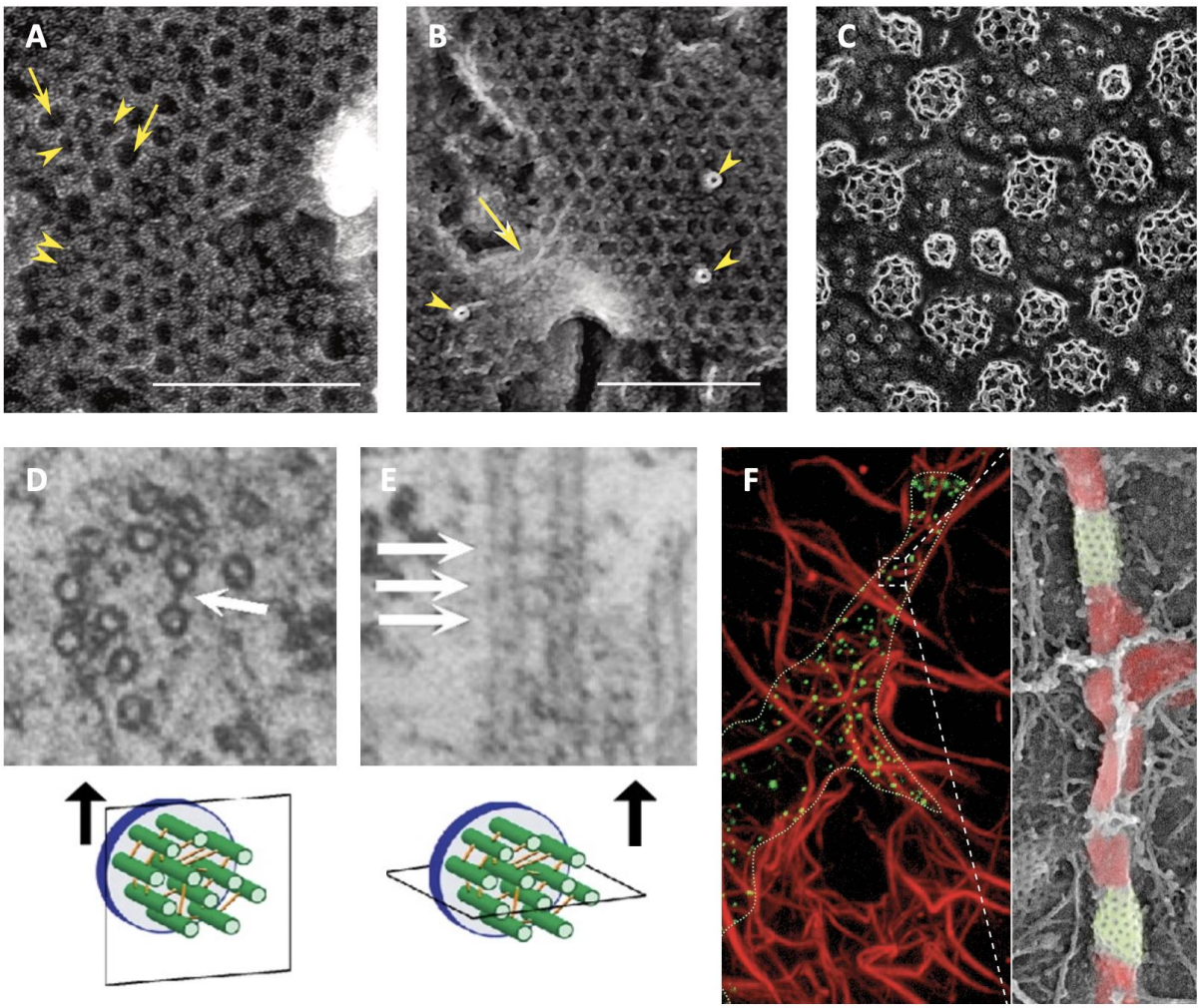


**Figure 5 – Clathrin structures in cells**

**EM images reproduced from published works demonstrating the different shapes clathrin complexes can make. A) Flat clathrin lattice formed primarily of hexagonal arrangements. Yellow arrows highlight other arrangements including pentagonal (arrowheads) and heptagonal (arrows). B) Flat clathrin lattices with a distorted or incomplete connecting lattice between the two, indicated by a yellow arrow, as well as possible attached remnants of cytoskeletal filaments, indicated by yellow arrowheads. A and B are reprinted from Akisaka et al (2021) (172) with permission from Elsevier. Scale bar represents 0.2 µm. C) Clathrin coated vesicles formed primarily in a pentagonal arrangement. Reproduced and adapted with permission from the Heuser lab. D&E) Orthogonal (D) and longitudinal (E) slices of kinetochore fibres, with bridges indicated by white arrows. It has been suggested that clathrin contributes to the composition of these bridges. Images are from Royle et al (2012) (173), reproduced and adapted with permission from The Company of Biologists Ltd. Original EM images from ©1970 Rockefeller University Press. Originally published in Hepler et al (1970) (174). F) Collagen fibres (red) with clathrin lattices (green) forming tubular structures around the fibers. From Elkhatib et al (2017) (175). Reproduced and adapted with permission from AAAS. Panels C-F: No scale bars were available from original publication.**

349 ## Synaptic Vesicle Recycling

350 Clathrin is essential for SV recycling during neurotransmission. Neurotransmission is the
351 process of transmitting a signal from one nerve cell to another through synapses, allowing
352 the sensory and nervous systems to communicate with one another. For neurotransmission
353 to occur, an action potential is generated: a short-lived rise and fall of a membrane's electrical
354 potential caused by $Na^+$ and $K^+$ transport across the membrane. Upon the action potential
355 reaching a synapse, calcium will flood into the pre-synaptic terminal and prompt SV's to fuse
356 with the plasma membrane and release the neurotransmitters found within them, allowing
357 the neurotransmitter to bind to receptors on the post-synaptic terminal to initiate an action
358 potential in the adjacent neuron. SV recycling is critical for maintaining the population of SV's
359 in neurons, with defects in SV recycling causing neurodegeneration and impaired neuronal
360 function (176).

361 Endophilin is a membrane binding protein that senses and generates curvature in cellular
362 membranes (66,122,177–179). It interacts with clathrin and other CME adaptors including
363 synaptojanin and dynamin, contributing both to clathrin-mediated endocytosis and a newly
364 identified form of endocytosis called fast endophilin-mediated endocytosis (FEME). While
365 clathrin is essential for synaptic vesicle regeneration, its precise role has been re-examined in
366 light of developments such as the identification of FEME and activity-dependent bulk
367 endocytosis (ADBE), reviewed in Chanaday et al 2019 J Neuroscience (180). CCV uncoating
368 has long been identified as an essential component of synaptic vesicle regeneration (178,181–
369 183) but further light has been shed on this by a report from Farsi et al 2018 that
370 reacidification of synaptic vesicles occurs rapidly following Hsc70-driven removal of clathrin
371 coats (184). Farsi et al propose a model whereby steric hindrance by the assembled clathrin

372 scaffold inhibits vATPase activity. This intriguing possibility further highlights the versatility
373 of clathrin in different functional contexts.

## 374 Hormone desensitisation

375 Hormone desensitisation is essential for controlling the cellular response to hormones in the
376 environment. Desensitisation follows sustained stimulation of receptors, leading them to lose
377 their ability to respond to the hormone. Clathrin-mediated endocytosis has been shown to
378 facilitate desensitisation through internalisation of a wide range of receptors, including the
379 parathyroid hormone receptor, β2-adrenergic receptor, and delta-opioid receptor (185–187).
380 In the case of G-protein-coupled receptors (GPCR) (188,189), desensitisation is mediated
381 through phosphorylation of the GPCRs, which often occurs within their C-terminal tail. This
382 stimulates arrestins (such as beta-arrestin) to bind to the GPCR, which prevents activation of
383 the associated G-protein and targets the GPCR for internalisation via CME through the
384 interaction of arrestin with the clathrin terminal domain and AP2 (190–194). It is now
385 understood that there are multiple routes for GPCR internalisation that employ both clathrin-
386 independent endocytic pathways and clathrin and AP-2 dependent, but arrestin-
387 independent, routes (195).

## 388 Spermiogenesis

389 Spermiogenesis must be performed to create functional sperm cells, which is the process of
390 forming matured elongated spermatids. CME is vital during spermiogenesis as it ensures germ
391 cells take up the proteins and molecules required to create components for the flagellum and
392 acrosome (196). For example, the spreading and shaping of the acrosome over the nucleus
393 and establishing distinct regions in the acrosome have been attributed to coated vesicle

394 formation at the acrosomes posterior and the trafficking of vesicles between the Golgi
395 apparatus and acrosome (197).

396 CME adaptors may also have other roles besides enabling CME during spermiogenesis.
397 Stromal membrane-associated protein 2 (SMAP2) is an ADP ribosylation factor (Arf) GTPase-
398 activating protein that interacts with CALM and clathrin. During spermiogenesis, SMAP2
399 deficiency impairs acrosome formation and nucleus reorganisation, and causes the trans-
400 Golgi network structure to be distorted and produce larger proacrosomal vesicles, as CALM is
401 not recruited to the trans-Golgi network. This suggests that CALM regulation of proacrosomal
402 vesicle size at the trans-Golgi network is vital for acrosome formation (198). Another example
403 involves endophilin. The endophilin III n-terminal BAR domain protein called endophilin A3
404 has been found to interact with the protein DPY30 domain-containing protein 1 (DYDC1),
405 which is exclusively expressed in the brain and testis and accumulates around the acrosome
406 during the late stages of spermiogenesis. Knockdown of DYDC1 negatively impacts acrosome
407 formation, suggesting that endophilin A3 and DYDC1 are required for acrosome formation
408 (199). Endophilin A3 has also been found to form a complex with activated epidermal growth
409 factor receptor and interact with Synaptojanin I, with endophilin A3, clathrin and
410 synaptojanin being colocalised in elongated spermatids (196). This evidence suggests that the
411 CME adaptors endophilin A3, Synaptojanin I, CALM, and clathrin are necessary for acrosome
412 development during spermatogenesis.

## 413 Collagen and Cell Migration

414 Clathrin's shape shifting ability is further illustrated in the context of cell migration. Regulation
415 of integrin endocytosis is required for adhesion disassembly and cell movement, which is
416 achieved through the recruitment of clathrin coated structures (CCS) to focal adhesions

417 (200,201). Focal adhesions form contacts between intracellular actin bundles and
418 extracellular substrates and are mostly observed at the extremities of elongated cells during
419 cell migration (202).

420 During cell migration, CCS's will also interact with collagen fibres. In comparison to other
421 areas of the cell, CCS's are found to nucleate preferentially along collagen fibres, and when in
422 contact with collagen fibres, CCS's are longer lived (175). As CCSs that interact with integrin
423 can form tight contacts with planar substrates (203,204), CCSs bound to collagen fibres allow
424 cells to anchor cellular protrusions to collagen fibres by forming tight contacts with integrin-
425 containing focal adhesions. Pinching of collagen fibres by CCSs may also create friction to help
426 cells produce long protrusions for cell migration (175). The clathrin-coated structures
427 identified by Elkhatib et al (2017) (175) showed previously unseen clathrin lattices with a
428 cylindrical shape, further emphasising the versatility of clathrin assemblies (See figure 5).

429 Elkhatib et al (2017) (175) also showed that the endocytic adaptors Disabled-2 (Dab2) and
430 AP2 were essential for cellular migration (175). Dab2 is required for recruiting integrins.
431 Silencing of Dab2 inhibits the clustering of integrins on CCS's, leading to reduced CCS lifetimes
432 on collagen fibres. This suggested that Dab2 and integrin are required for balancing out
433 budding forces created by CCS's on collagen fibres. Silencing of Dab2 and AP2 also caused a
434 more pronounced retraction of cellular protrusions, further supporting the idea that CCSs
435 stabilise cellular protrusions by anchoring collagen fibres to focal adhesions, allowing cells to
436 sustain high tension and form long protrusions during cell migration (175).

437 ## Mitosis

438 Perhaps one of the more unusual roles clathrin adopts in cells is in mitosis, since here its
439 function does not appear to be associated with the formation of the curved or planar lattices
440 that have become a hallmark of clathrin function in other contexts. In mitosis, a cell divides
441 into two identical daughter cells. To carry this out, mitotic spindles attach to the kinetochore
442 complex on chromosomes and bring the chromosomes together. The chromosomes are then
443 aligned during the metaphase stage and segregated towards the poles of the cell during the
444 anaphase stage. Clathrin has been found to colocalise alongside tubulin at mitotic
445 spindles (18,173,205–207). The mitotic spindle requires the presence of clathrin triskelia
446 which have been shown to stabilise kinetochore fibres (18,208–210). The N-terminal domains
447 of clathrin are responsible for interactions between clathrin and microtubules within the
448 mitotic spindle. The bridge hypothesis suggests that clathrin increases kinetochore stability
449 by bracing between two to three microtubules within a kinetochore fibre, which is possible
450 due to its trimeric structure. Experiments using clathrin constructs with altered trimeric
451 structural properties have shown that clathrin triskelia's native structure is vital for its
452 stabilising function during metaphase and anaphase (209). CHC acts with transforming acidic
453 coiled-coil containing protein 3 (TACC3) and colonic hepatic tumour overexpressed gene (ch-
454 TOG; also known as cytoskeleton-associated protein 5, CKAP5) in performing this function.
455 Depletion of CHC has been found to stop TACC3 relocation to the mitotic spindle, which
456 causes disorganised spindles and chromosome misalignment (211). Recent work by Rondelet
457 et al 2020 (212) has identified an additional protein in this complex, GTSE1, which binds to
458 clathrin via the N-terminal domain and inhibits the microtubule depolymerase MCAK. This

459 discovery directly links clathrin-adaptor interactions classically associated with endocytosis,
460 with stabilisation of microtubules during mitosis.

461 Interestingly, the clathrin light chain subunit, CLCa, also interacts with mitosis adaptors, such
462 as mitotic arrest deficient 2-like protein 2 (MAD2B). MAD2B binds to the proteins cell division
463 cycle protein 20 homolog (CDC20) and or cadherin-1 to inhibit the anaphase promoting
464 complex, and colocalise at the mitotic spindle. Depletion of MAD2B stops CLCa from being
465 concentrated at the mitotic spindle, which inevitably leads to an increase in misaligned
466 chromosomes (208). The precise structures that clathrin adopts when associated with
467 kinetochores have not yet been determined. However, the current morphological
468 information available suggests that any structure adopted by clathrin is likely to differ from
469 the classical polyhedral arrays seen in clathrin-coated vesicles and flat lattices, since such
470 structures have not been observed in mitotic spindles (213).

## 471 Pathogen entry into cells facilitated by clathrin

472 One more dramatic form of shape-shifting performed by clathrin is in engulfment of large
473 cargoes, and particularly microorganisms. Early studies showed that large areas of the plasma
474 membrane surrounding vesicular stomatitis virus exhibited a clathrin coat as demonstrated
475 in figure 6A and 6B, and that internalisation depended on clathrin (214–217). Since then,
476 many viruses have been shown to enter cells by endocytosis, many through clathrin-
477 dependent pathways (218). Viruses present a sizeable cargo, but in 2005 it was shown that
478 clathrin was essential for the internalisation of an even larger cargo, the bacterium *Listeria*
479 *monocytgenes*, which can reach lengths of 2 – 6 µm long (219–222). This led to further
480 discoveries of a requirement for clathrin in internalisation of other bacteria including S.

481 *aureus* and Enteropathogenic *E. coli* (EPEC), and the fungal pathogen *Candida albicans*

482 (220,221,223–226).

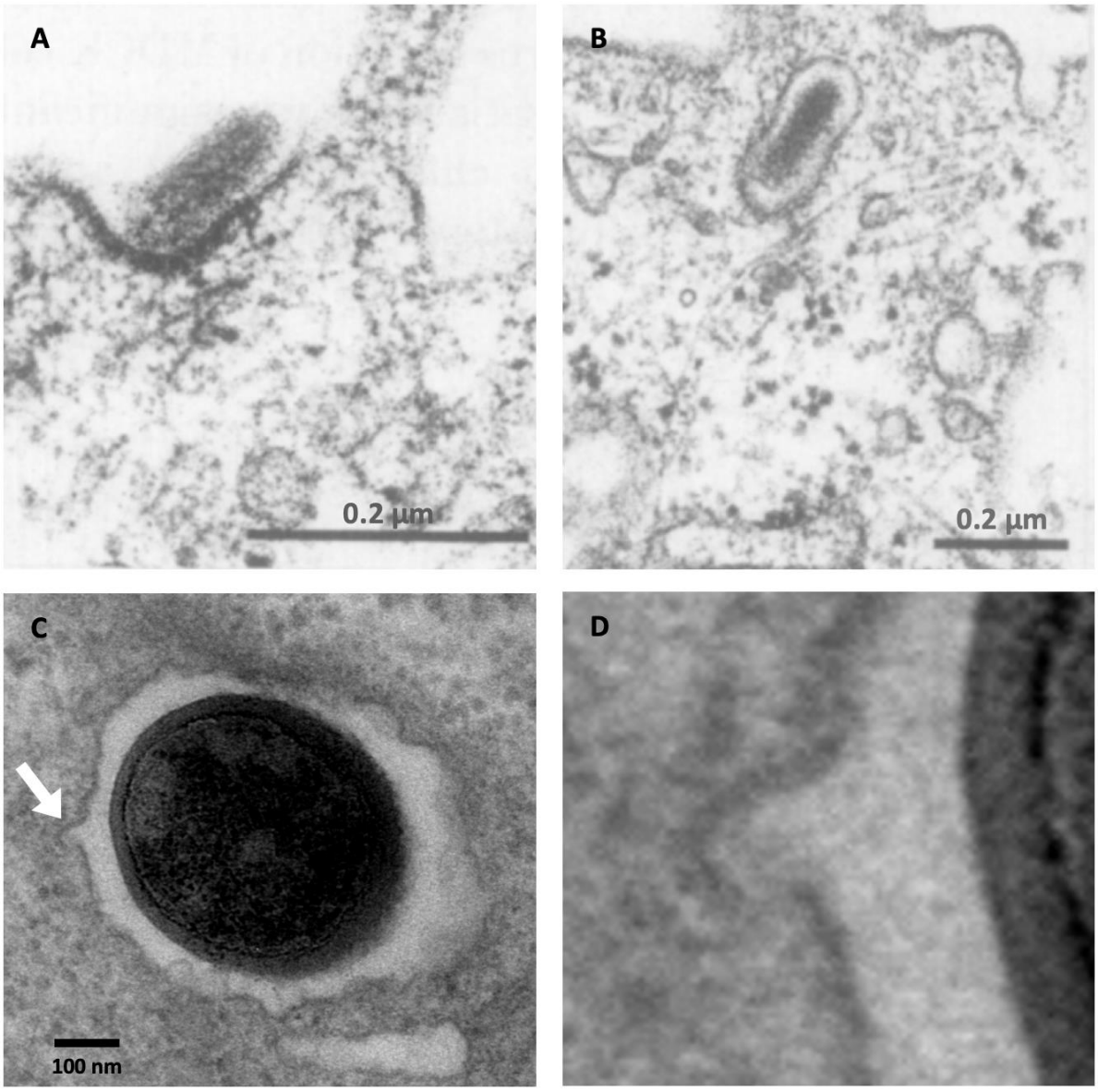


483

484 **Figure 6 – Early images of viral entry into cells**

485 **TEM images of CME during viral entry. A and B) CME of vesicular stomatitis virus in MDCK cells. A) CCV**
486 **formation around virus. B) Partially coated CCV around internalised virus. A and B reprinted from Matlin et al**
487 **(1982) (217) with permission from Elsevier. C) and D) Formation of clathrin-coated structures during infection**
488 **of Jeg3 cells by L. monocytogenes. The arrow points to a clathrin-coated structure close to the internalised**
489 **bacterium. This is shown as an enlarged view in D. Image was provided by M. Bonazzi and P. Cossart and**
490 **adapted by permission.**

491 Bonazzi et al (2011) (221) investigated the mechanism by which clathrin might be employed

492 to engulf cargo of such a size. Observations from electron microscopy images of cells

493 undergoing infection by either *Listeria* or enteropathogenic *E. coli* (EPEC) showed that
494 complete clathrin-coated vesicles were not observed in the vicinity of the bacterium. Rather
495 clathrin-coated pits, of a size and shape similar to those observed in uninfected cells, were
496 seen in the membrane surrounding the bacterium. Immunolabelling of clathrin in HeLa cells
497 infected with *L. monocytogenes* showed that it was always associated with curved
498 invaginations, and was not seen in areas where the membrane was flat. In the case of EPEC-
499 infected cells, clathrin in the vicinity of EPEC-induced actin pedestals also appeared in the
500 form of coated pits rather than complete vesicles. Further investigations by Bonazzi et al
501 (2011) showed that coated pit formation required the adaptor Dab2 and this in turn
502 facilitated recruitment of actin via Hip1R and the clathrin light chain. Actin recruitment
503 depended on tyrosine phosphorylation of the clathrin heavy chain. Once assembled, this
504 machinery was then able to recruit the motor protein Myosin VI which could provide a pulling
505 force. Thus, in an alternative form of shape-shifting, the invading bacterium triggers clathrin
506 and its associated machinery to organise actin to generate structures that facilitate uptake of
507 a cargo far exceeding the size of a clathrin-coated vesicle.

508 ## GLUT4 Trafficking and the role of CHC22

509 So far we have discussed the action of clathrin that in humans is encoded by the gene CLTC
510 on chromosome 17 and is termed CHC17. However, in jawed vertebrates there is a second
511 form of clathrin, CHC22, encoded by the gene CLTCL1 on chromosome 22 (227,228). This form
512 of clathrin is expressed most highly in muscle and adipose tissue and has been shown to play
513 a key role in transport of insulin-regulated glucose transporter 4 (GLUT4). GLUT4 is a glucose
514 transporter found in adipocyte and muscle cells which is transported to the cells plasma
515 membrane upon insulin signalling (229,230). This is achieved through sorting of GLUT4 into

516 insulin-responsive vesicles for selective transport (230). CHC22 interacts with GLUT4 as well
517 as the ER-to-Golgi intermediate compartment (ERGIC) tether p115, sortilin, IRAP, and GGA2
518 to sort GLUT4 in the GLUT4 storage compartment in cells (229,231). Unlike CHC17 which is
519 involved in CME and other cellular pathways like mitosis and cell migration, CHC22 is limited
520 to retrograde sorting as it does not support vesicle formation at the plasma membrane in the
521 presence or absence of CHC17, and also forms a more stable coat which cannot be removed
522 by the same disassembly complex used to remove CHC17 (229,232). CHC22 is also restricted
523 in its tissue and species expression, whereas CHC17 is not (229). Several studies however have
524 suggested another role for CHC22 besides sorting GLUT4 involving the initiation of GLUT4
525 sequestration upon an insulin response. Downregulation of either p115 or CHC22 reduces
526 trafficking of GLUT4 to the plasma membrane, suggesting CHC22 initiates GLUT4
527 sequestration from the ERGIC in humans and conducts retrograde sorting of GLUT4 (231).
528 Additionally, functional studies of different CHC22 allotypes identified differences in GLUT4
529 transport in response to insulin; these results suggested that changes in diet (i.e. a shift from
530 eating mostly meat to more plant-based foods) have impacted the allotype of CHC22 selected
531 in humans, causing an alteration in the effectiveness of CHC22's role in insulin-regulated
532 GLUT4 transport (227). Further studies on the mechanism by which CHC22 sorts and
533 transports GLUT4, as well as structural studies on a CHC22 coat that might explain its
534 additional stability are needed to determine how this different form of clathrin CHC
535 contributes to its more specialised function (227,229–232).

536 # Clathrin shapeshifting

537 ## Clathrin exchange and the dynamic coat assembly model

538 Clathrin is remarkable for its ability to form both planar and curved lattice structures within
539 its diverse cellular roles. This has led to debate about how, or whether these clathrin lattice
540 structures might shapeshift to form planar or curved arrangements. High energy costs have
541 been predicted for remodelling of a planar clathrin lattice to a curved CCP due to the
542 structural rearrangements between triskelion leg contacts that would be required (233,234).
543 Two models have emerged within this debate (235). The first has been termed the 'constant
544 curvature' model, in which clathrin assembles into a curved lattice as the membrane
545 invaginates to form a CCP (19,236). In the second 'dynamic coat' or 'constant area' model,
546 the area of membrane coated by the clathrin lattice remains constant during budding while
547 curvature increases (19,233,234,237–239). These two models of CCV formation are
548 demonstrated in figure 7A.

549 One means proposed by which a planar clathrin lattice could transform into a curved lattice
550 involves dynamic exchange of clathrin between the invaginating membrane and a soluble
551 pool of clathrin triskelia (96,240). The mechanism by which this exchange could take place
552 may utilise the coated vesicle uncoating apparatus of ATP-dependent clathrin disassembly by
553 Hsc70, recruited to the vesicle by auxilin/GAK, and there is experimental evidence supporting
554 this (139,241–243). Exchange of clathrin in a 'wrong' conformation for new clathrin able to
555 adopt a 'right' conformation that is fuelled by an existing ATP-driven system for clathrin
556 disassembly neatly addresses the question of how established planar lattices could be
557 remodelled to produce a curved coated pit (98,238,241,244). However, arguing against this

558 is the observation that in genome-edited cells, endogenously labelled auxilin and GAK could

559 not be detected during the early stages of vesicle development (132).

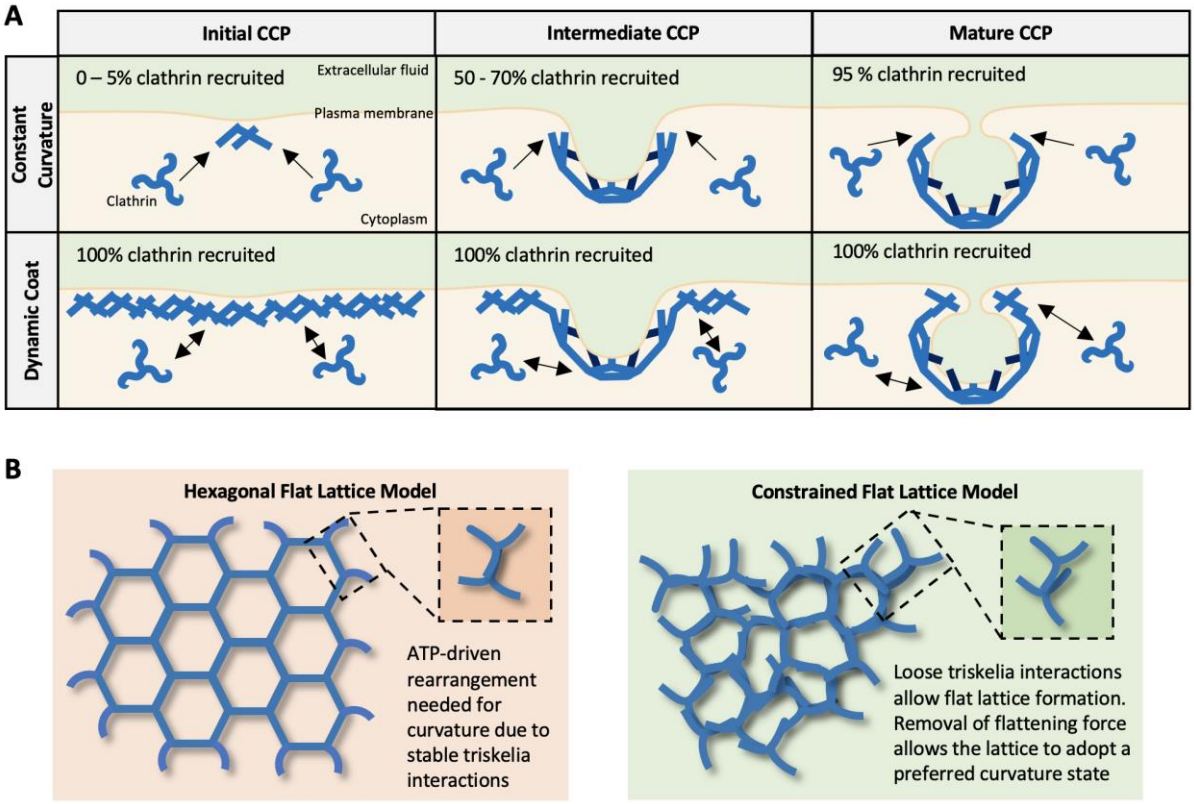


560

561 **Figure 7 – Models for CCV and flat lattice formation**

562 **Schematic diagrams demonstrating models for CCV and flat lattice formation. A) Two models for CCV**
563 **formation, including the constant curvature model where no clathrin exchange occurs, and the dynamic coat**
564 **model where all clathrin is recruited into a lattice prior to membrane bending and requires clathrin**
565 **exchange for curvature formation. B) Comparison of the hexagonal flat lattice model with the constrained**
566 **flat lattice model proposed by Sochaki et al (2020) (245).**

567 A planar lattice is not, however, the only route to clathrin-coated vesicle formation. Clathrin-

568 coated structures have been observed in a number of systems (108,246–248) to have formed

569 independently, suggesting that a planar lattice is not a prerequisite for generation of

570 curvature. Indeed, curved clathrin lattices have been shown to form spontaneously both in

571 vitro and in unroofed cells (31,245) suggesting that lattice remodelling may not be essential

572 in coated vesicle formation.

573 Evidence in support or otherwise of mechanisms for achieving clathrin modelling has been
574 carefully discussed in several reviews (16,19,235) but as some authors point out (19,235) it
575 seems likely that there are multiple routes to curvature. Such alternative routes may be
576 influenced by the need to regulate import of cargo, as shown by Maib *et al* (2018) (249). In
577 this study, the import of the GPCR P2Y12 into neuronal cells differed from that of transferrin
578 in requiring clathrin rearrangement dependent on phosphorylation of CLCb and the presence
579 of auxilin. This suggested that different modes of lattice formation may be required for certain
580 cargos, which in turn could provide additional layers of control for their uptake.

581 Interestingly, recent work from Sochacki et al (2020) presents a comprehensive analysis of
582 the morphology of clathrin lattices seen in eight different mammalian cell lines (245). As a
583 result of this analysis the authors propose a new model for clathrin coated vesicle formation
584 whereby the potential to form curved structures is 'pre-programmed' within a planar lattice.
585 This model is based on new structural detail obtained using cryo-electron tomography that
586 has revealed irregular structures within planar lattices showing the potential for curved
587 structures to form upon release of constraints holding the planar lattice in place (245). This is
588 in contrast to previous assumptions that such lattices would be fully formed hexagonal arrays,
589 upon which energetic calculations for changes in morphology had been based (233,234).
590 Figure 7B demonstrates the differences between the old and new models. This model
591 suggests a new way to see clathrin shape-shifting – as the outcome of the balance achieved
592 between opposing forces generated through interactions between membrane, adaptors and
593 clathrin, membrane tension and the mechanical properties of these components.

## A structural basis for clathrin shape-shifting

This review has so far focussed on the way that clathrin participates in cellular processes and in the involvement of binding partners in formation of multiple clathrin lattices. But clathrin is able to adopt different shapes in the absence of other cellular components, as shown in early studies (35,36,250–253) where multiple cage arrangements similar to those observed in coated vesicles could be induced using only purified protein (254). Later studies showed that clathrin could also adopt more unusual conformations such as cube arrangements (shown in Figure 8) and tetrahedral cages (255,256). On the other hand, formation of biochemically generated flat lattices seemed to require involvement of additional support such as stabilisation of clathrin association with a flat surface or membrane through use of an adaptor protein (31,92,257). Thus, in this final section we discuss how the structural properties of clathrin itself lead to formation of multiple distinct lattice arrangements.

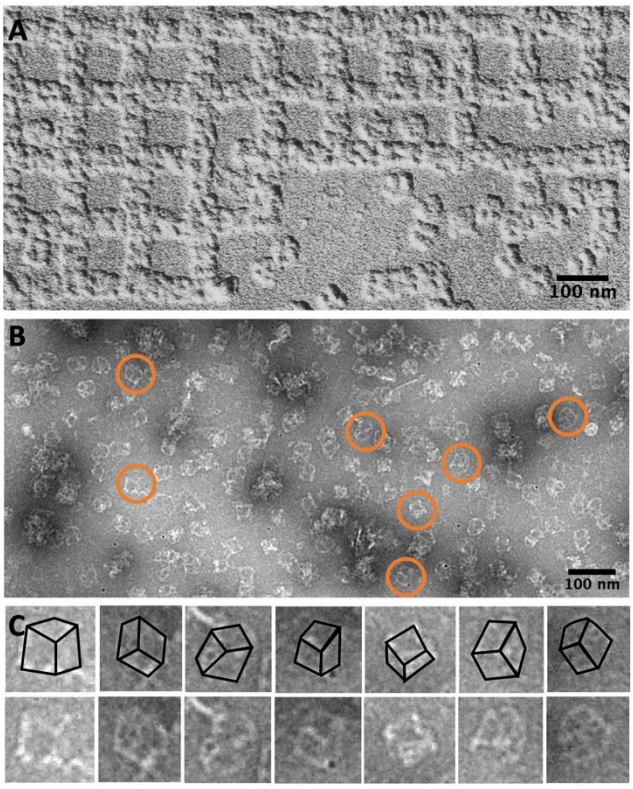

**Figure 8 – Cube lattice structures formed by clathrin in vitro**

**Unusual structures formed from clathrin triskelia in vitro. A) Electron micrograph of clathrin cubes that have formed into an open square-packed array. Image provided by R. A. Crowther. B and C) Clathrin cube structures imaged by negative stain electron microscopy. Circled cubes in B have been enlarged and presented in C alongside fitted schematics of clathrin cubes to the images. Image provided by and adapted with permission from M. Halebian (Smith lab).**

The mechanical properties of clathrin are determined by the tertiary structure of the CHC legs which are composed of pairs of short, stacked alpha helices, and the strong association of the CLC long helix which acts as a brace, giving strength and rigidity to the triskelion leg (92,233,234,258–261). The trimerization domain, strengthened by additional helices contributed by the light chain c-terminus, joins three CHC subunits together via a highly stable interaction to form the triskelion structure that serves as clathrin's smallest functional structural unit in classical clathrin lattices (260–263). The arrangement of alpha helices in stacked pairs within the heavy chain leg seems to confer flexibility to the leg, as with the coils in a spring, that is then braced where the light chain binds. This is supported by structural studies showing that in conformations adopted by triskelion legs within a cage, most flexibility is seen beyond the reach of the bound light chain (41,264). Further, the mode of binding of the light chains has been shown to influence heavy chain conformation (261) and a recent study has demonstrated a role for the light chain in controlling how clathrin deforms lipid membrane. Redlinghofer et al (2020) (93) showed that the quality of clathrin lattices and the size and shape of clathrin-coated buds varied according to the composition of CLC isoforms a and b, and their neuronal splice variants, suggesting a means by which lattice size and shape could be controlled to meet the needs of the cell.

The relationship between leg conformation and lattice structure was explored by Morris et al (2019) (41) who determined cryo-EM structures for 5 different types of cage arrangement, with three of these at sufficient resolution to support further analysis. Superimposition of

633 the paths adopted by triskelion legs in several different cage forms showed that the leg
634 shapes varied most through changes in the angle between the CHC distal joint and distal
635 domain, ranging between 7° and 17°. Furthermore, the shapes of legs from similar types of
636 local structure (e.g. a hexagonal or pentagonal face) could not always be superimposed, and
637 no pattern between the leg angles adopted and the type of local structure formed could be
638 seen. This suggested there were multiple ways in which legs could come together to arrive
639 at the same overall cage structure. In contrast, however, no significant differences in
640 intermolecular contact patterns were observed at the resolutions obtained, regardless of the
641 type of local structure formed. This suggested that clathrin triskelia adopt a universal mode
642 of assembly, and that multiple combinations of particular leg conformations can lead to
643 structures with the same lattice geometry through adaptation of the shape of one leg to that
644 of another (41). Thus, assuming the energetic requirements of rearranging contacts could be
645 met, clathrin seems to be uniquely adapted to being able to transition from planar to curved
646 lattices simply through making relatively small changes in the leg angles adopted by clathrin
647 triskelia. This in turn allows clathrin molecules to accommodate varying curvature and
648 differing local geometric environments.

## 649 Conclusions

650 Clathrin's unusual structure and capacity to assemble into multiple lattice types gives it a
651 remarkable 'shape-shifting' ability. In addition to forming lattices, clathrin is also able to bind
652 multiple partners via its terminal domains. Lattice assembly together with coordination of
653 multiple protein-protein interactions fits clathrin for multiple roles within cells. The best-
654 known function is the formation of clathrin-coated vesicles which are employed in a variety
655 of contexts including absorption of nutrients and other required molecules at the plasma

656 membrane, receptor down-regulation, intracellular trafficking, synaptic vesicle recycling and
657 spermiogenesis. The precise nature of the shape shifting required to achieve coated vesicle
658 formation is still debated, but advances in cryo-electron tomography and correlative light and
659 electron microscopy techniques, large scale statistical analyses and single molecule light
660 microscopy are revealing these processes in increasing detail (48,132,245,265,266), and
661 recent developments in time-resolved cryo-electron microscopy may enable the capture of
662 conformational changes in clathrin and its assemblies on a millisecond timescale (267).

663 Alongside formation of clathrin-coated vesicles, clathrin forms other structures with different
664 roles. The prevalence of flat clathrin lattices, or plaques, in cells has recently been termed
665 'frustrated endocytosis'. Roles in signal transduction, cell migration and cell adhesion have
666 been proposed and recently tubular clathrin structures have been observed around collagen
667 fibres. These lattices appear to lend a stabilising force in situations where the cell makes
668 contact with a surface, a large potential cargo, or neighbouring cells. These examples
669 illustrate the versatility of the clathrin structure for different cellular roles and in these cases
670 clathrin is seen to form different lattice morphologies. However, in the case of mitosis the
671 situation appears to be different. Clathrin has been shown to stabilise the kinetochore within
672 the mitotic spindle but so far none of the commonly observed clathrin lattices have been
673 observed, suggesting that the shape adopted by clathrin in this role is unlike the classic
674 polyhedral lattices we commonly see.

675 In conclusion, we see clathrin able to form a remarkable range of lattice structures in cells,
676 and within different functions. At the core of this lies the ability of clathrin molecules to
677 flexibly adapt to the shape of a neighbouring triskelion leg, whilst maintaining a universal
678 mode of assembly. Discussion continues as to how these structures are formed but

679 comprehensive studies of different cell types combined with high resolution structural
680 analysis show promise in addressing the many questions such structural arrangements pose.

## 681 Competing Interests

682 The authors declare that there are no competing interests associated with the manuscript.

## 683 Data Availability

684 Molecular models 1B89, 1XI5, 6SCT, 1BPO, 3IYV used in the production of Figure 2 can be
685 found at Protein Data Bank in Europe (PDBe) at https://www.ebi.ac.uk/pdbe/.

686 EM maps EMD-5119 and EMD-0126 used in the production of Figure 2 can be found at the
687 Electron Microscopy Data Bank (EMDB) at PDBe:
688 https://www.ebi.ac.uk/pdbe/emdb/index.html.

## 689 Acknowledgements

690 KMW is funded by MRC Doctoral Training Partnership grant MR/N014294/1.
691 CJS thanks BBSRC [grant no. BB/N008391/1] for support and the Royal Society and
692 Leverhulme Trust for a Senior Research Leave Fellowship. We thank S J Royle for helpful
693 comments on the manuscript.

## 694 Abbreviations

695 ADBE – Activity-dependent bulk endocytosis

696 ADP – Adenosine diphosphate

697 AP1 – Adaptor protein 1

698 AP180 – Assembly protein 180 kDa

699 AP2 – Adaptor protein 2

700 Arf – ADP ribosylation factor

701 ATP – Adenosine triphosphate

702 BAR – Bin/Amphiphysin/Rvs

703 CALM – Clathrin-assembly lymphoid myeloid leukaemia protein

704 CCP – Clathrin coated pit

705 CCS – Clathrin coated structure

706 CCV – Clathrin coated vesicle

707 CDC20 – Cell division cycle protein 20 homolog

708 CHC – Clathrin heavy chain

709 ch-TOG – Colonic hepatic tumour overexpressed gene

710 CKAP5 – Cytoskeleton-associated protein 5

711 CLC – Clathrin light chain

712 CME – Clathrin mediated endocytosis

713 Dab2 – Disabled-2

714 DYDC1 – DPY30 domain-containing protein 1

715 Eps15 – Epidermal growth factor receptor substrate 15

716 Eps15R – Epidermal growth factor receptor substrate 15 receptor

717 FEME – Fast endophilin-mediated endocytosis

718 FBXO32 – F-Box Protein 32

719 FCHo1/2 – Fer/Cip4 homology domain-only proteins 1 and 2

720 FRAP – Fluorescence recovery after photobleaching

721 GAK – Cyclin G-associated kinase

722 GHSR-1a – GH secretagogue receptor subtype 1a

723 GPCR – G-protein coupled receptor

724 HIP1R – Huntington-interacting protein 1-related protein

725 Hsc70 – Heat shock cognate 71 kDa protein

726 Hsp110 – Heat shock protein 110

727 LϕXϕ[DE] – L(L, I)(D, E, N)(L, F)(D, E)

728 MAD2B – Mitotic arrest deficient 2-like protein 2

729 OCRL1 – Oculocerebrorenal syndrome of Lowe protein 1

730 PDB – Protein Data Bank

731 PI(4,5)P2 – Phosphatidylinositol 4,5-bisphosphate

732 PTEN – Phosphatase and tensin homolog deleted on chromosome ten

733 RME – Receptor mediated endocytosis

734 SMAP2 – Stromal membrane-associated protein 2

735 SNX9 – Sorting Nexin 9

736 SV – Synaptic vesicle

737 TACC3 – Transforming acidic coiled-coil containing protein 3

738 TIRF – Total internal reflection fluorescence

739

740

741 **Legends to Figures**

742 **Figure 1 – Clathrin-mediated endocytosis in cellular processes**

743 Schematic diagram demonstrating the variety of cellular processes in which clathrin is used, including but not
744 limited to endocytosis, spermiogenesis, cell migration, hormone desensitisation, mitosis, and SV recycling (1–
745 4,14–19). Diagram is not to scale.

746 **Figure 2 – Clathrin structure**

747 A) Domain organisation within CLC and CHC (41). B) Model of a clathrin triskelion including the bovine CHC
748 model (Protein Data Bank (PDB): 3IYV) (37) informed by fitting the high resolution x-ray structure (PDB: 1B89)
749 (42) into cryo-EM density maps and the porcine CLC model produced from cryo-EM density maps (PDB: 6SCT)
750 (41). C) Model of a bovine clathrin cage (EMD: 5119) with fitted clathrin triskelion model produced from cryo-
751 EM density maps (PDB: 1XI5) (37). D) Recent 4.7 Å porcine clathrin hub structure with fitted PDB model (PDB:
752 6SCT) produced from cryo-EM density maps (EMD: 0126) (41). E) Model of a rat CHC terminal domain
753 produced from x-ray diffraction density (PDB: 1BPO), with location of binding sites for different motifs
754 highlighted (43). All structure visualization was performed with UCSF Chimera (44).

755 **Figure 3 – Stages in clathrin mediated endocytosis**

756 Schematic diagram illustrating different stages in CME, including A) nucleation and assembly, followed by B)
757 stabilisation and maturation, followed by C) constriction and scission, followed by D) clathrin uncoating. Figure
758 is not to scale.

759 **Figure 4 – Models for clathrin cage disassembly**

760 Schematic diagram demonstrating two different models for hsc70 driven disassembly of clathrin cages,
761 including A) the steric wedge/Brownian ratchet model, and B) the wrecking ball/entropic pulling model.
762 Diagram is not to scale.

763 **Figure 5 – Clathrin structures in cells**

764 EM images reproduced from published works demonstrating the different shapes clathrin complexes can
765 make. A) Flat clathrin lattice formed primarily of hexagonal arrangements. Yellow arrows highlight other
766 arrangements including pentagonal (arrowheads) and heptagonal (arrows). B) Flat clathrin lattices with a
767 distorted or incomplete connecting lattice between the two, indicated by a yellow arrow, as well as possible
768 attached remnants of cytoskeletal filaments, indicated by yellow arrowheads. A and B are reprinted from
769 Akisaka et al (2021) (172) with permission from Elsevier. Scale bar represents 0.2 µm. C) Clathrin coated
770 vesicles formed primarily in a pentagonal arrangement. Reproduced and adapted with permission from the
771 Heuser lab. D&E) Orthogonal (D) and longitudinal (E) slices of kinetochore fibres, with bridges indicated by
772 white arrows. It has been suggested that clathrin contributes to the composition of these bridges. Images are
773 from Royle et al (2012) (173), reproduced and adapted with permission from The Company of Biologists Ltd.
774 Original EM images from ©1970 Rockefeller University Press. Originally published in Hepler et al (1970) (174).
775 F) Collagen fibres (red) with clathrin lattices (green) forming tubular structures around the fibers. From
776 Elkhatib et al (2017) (175). Reproduced and adapted with permission from AAAS. Panels C-F: No scale bars
777 were available from original publication.

778 **Figure 6 – Early images of viral entry into cells**

779 TEM images of CME during viral entry. A and B) CME of vesicular stomatitis virus in MDCK cells. A) CCV formation
780 around virus. B) Partially coated CCV around internalised virus. A and B reprinted from Matlin et al (1982) (217)
781 with permission from Elsevier. C) and D) Formation of clathrin-coated structures during infection of Jeg3 cells by
782 L. monocytogenes. The arrow points to a clathrin-coated structure close to the internalised bacterium. This is
783 shown as an enlarged view in D. Image provided by M. Bonazzi and P. Cossart and adapted by permission.

784 **Figure 7 – Models for CCV and flat lattice formation**

785 Schematic diagrams demonstrating models for CCV and flat lattice formation. A) Two models for CCV
786 formation, including the constant curvature model where no clathrin exchange occurs, and the dynamic coat
787 model where all clathrin is recruited into a lattice prior to membrane bending and requires clathrin exchange
788 for curvature formation. B) Comparison of the hexagonal flat lattice model with the constrained flat lattice
789 model proposed by Sochaki et al (2020) (245).

790 **Figure 8 – Cube lattice structures formed by clathrin in vitro**

791 Unusual structures formed from clathrin triskelia in vitro. A) Electron micrograph of clathrin cubes that have
792 formed into an open square-packed array. Image provided by R. A. Crowther. B and C) Clathrin cube structures
793 imaged by negative stain electron microscopy. Circled cubes in B have been enlarged and presented in C
794 alongside fitted schematics of clathrin cubes to the images. Image provided by and adapted with permission
795 from M. Halebian (Smith lab).

796

797 ## References


798 1. Baschieri F, Porshneva K, Montagnac G. Frustrated clathrin-mediated endocytosis –
799 causes and possible functions. J Cell Sci. 2020;133(11). DOI: 10.1242/jcs.240861.

800 2. Doherty GJ, McMahon HT. Mechanisms of Endocytosis. Annu Rev Biochem.
801 2009;78(1):857–902. DOI: 10.1146/annurev.biochem.78.081307.110540.

802 3. Mayor S, Parton RG, Donaldson JG. Clathrin-Independent Pathways of Endocytosis.
803 Cold Spring Harb Perspect Biol. 2014;6(6):a016758. DOI:
804 10.1101/cshperspect.a016758.

805 4. Mettlen M, Loerke D, Yarar D, Danuser G, Schmid SL. Cargo- and adaptor-specific
806 mechanisms regulate clathrin-mediated endocytosis. J Cell Biol. 2010;188(6):919–33.
807 DOI: 10.1083/jcb.200908078.

808 5. Garrett WS, Mellman I. Studies of endocytosis. In: Lotze MT, Thomson AW, editors.
809 Dendritic Cells. 2nd editio. Academic Press; 2001. p. 213–29. DOI: 10.1016/b978-
810 012455851-9/50055-9.

811 6. Stillwell W. Membrane Transport. In: An Introduction to Biological Membranes.
812 Elsevier; 2016. p. 423–51. DOI: 10.1016/b978-0-444-63772-7.00019-1.

813 7. Cullen PJ, Steinberg F. To degrade or not to degrade: mechanisms and significance of
814 endocytic recycling. Nat Rev Mol Cell Biol. 2018;19(11):679–96. DOI: 10.1038/s41580-
815 018-0053-7.

816 8. Bitsikas V, Corrêa IR, Nichols BJ. Clathrin-independent pathways do not contribute

817 significantly to endocytic flux. Elife. 2014;2014(3):1–26. DOI: 10.7554/elife.03970.

818 9. Roth TF, Porter KR. Yolk protein uptake in the oocyte of the Mosquito Aedes Aegypti.
819 L. J Cell Biol. 1964;20(2):313–32. DOI: 10.1083/jcb.20.2.313.

820 10. Pearse BMF. Coated vesicles from pig brain: Purification and biochemical
821 characterization. J Mol Biol. 1975;97(1):93–8. DOI: 10.1016/s0022-2836(75)80024-6.

822 11. Kaksonen M, Roux A. Mechanisms of clathrin-mediated endocytosis [Internet]. Vol.
823 19, Nature Reviews Molecular Cell Biology. Nature Publishing Group; 2018. p. 313–26.
824 DOI: 10.1038/nrm.2017.132.

825 12. Zhang B, Koh YH, Beckstead RB, Budnik V, Ganetzky B, Bellen HJ. Synaptic Vesicle Size
826 and Number Are Regulated by a Clathrin Adaptor Protein Required for Endocytosis.
827 Neuron. 1998;21(6):1465–75. DOI: 10.1016/s0896-6273(00)80664-9.

828 13. Miller SE, Mathiasen S, Bright NA, Pierre F, Kelly BT, Kladt N, Schauss A, Merrifield CJ,
829 Stamou D, Höning S, Owen DJ. CALM Regulates Clathrin-Coated Vesicle Size and
830 Maturation by Directly Sensing and Driving Membrane Curvature. Dev Cell.
831 2015;33(2):163–75. DOI: 10.1016/j.devcel.2015.03.002.

832 14. Wideman JG, Leung KF, Field MC, Dacks JB. The Cell Biology of the Endocytic System
833 from an Evolutionary Perspective. Cold Spring Harb Perspect Biol. 2014;6(4):a016998.
834 DOI: 10.1101/cshperspect.a016998.

835 15. Ho H-C. Clathrin-Coated Vesicles Leaving the Caudal Margin of the Developing
836 Acrosome Facilitate Acrosomal Shaping During Mouse Spermiogenesis. Biol Reprod.
837 2008;78(Suppl_1):218–218. DOI: 10.1093/biolreprod/78.s1.218b.

838 16. Sochacki KA, Taraska JW. From Flat to Curved Clathrin: Controlling a Plastic Ratchet
839 [Internet]. Vol. 29, Trends in Cell Biology. 2019. p. 241–56. DOI:
840 10.1016/j.tcb.2018.12.002.

841 17. Wecker L. Receptor Regulation. In: xPharm: The Comprehensive Pharmacology
842 Reference. Elsevier; 2007. p. 1–5. DOI: 10.1016/b978-008055232-3.60004-2.

843 18. Royle SJ, Bright NA, Lagnado L. Clathrin is required for the function of the mitotic
844 spindle. Nature. 2005;434(7037):1152–7. DOI: 10.1038/nature03502.

845 19. Briant K, Redlingshöfer L, Brodsky FM. Clathrin's life beyond 40: Connecting
846 biochemistry with physiology and disease. Curr Opin Cell Biol. 2020;65:141–9. DOI:
847 10.1016/j.ceb.2020.06.004.

848 20. Smith SM, Baker M, Halebian M, Smith CJ. Weak molecular interactions in clathrin-
849 mediated endocytosis. Front Mol Biosci. 2017;4(72). DOI: 10.3389/fmolb.2017.00072.

850 21. Goldstein JL, Brown MS, Anderson RGW, Russell DW, Schneider WJ. Receptor-
851 Mediated Endocytosis: Concepts Emerging from the LDL Receptor System. Annu Rev
852 Cell Biol. 1985;1(1):1–39. DOI: 10.1146/annurev.cb.01.110185.000245.

853 22. McMahon HT, Boucrot E. Molecular mechanism and physiological functions of
854 clathrin-mediated endocytosis. Nat Rev Mol Cell Biol. 2011;12(8):517–33. DOI:
855 10.1038/nrm3151.

856 23. Zhang F, Zang T, Wilson SJ, Johnson MC, Bieniasz PD. Clathrin Facilitates the
857 Morphogenesis of Retrovirus Particles. Luban J, editor. PLoS Pathog.
858 2011;7(6):e1002119. DOI: 10.1371/journal.ppat.1002119.

859 24. Song L, He Y, Ou J, Zhao Y, Li R, Cheng J, Lin CH, Ho MS. Auxilin Underlies Progressive
860 Locomotor Deficits and Dopaminergic Neuron Loss in a Drosophila Model of
861 Parkinson's Disease. Cell Rep. 2017;18(5):1132–43. DOI:
862 10.1016/j.celrep.2017.01.005.

863 25. Nguyen M, Krainc D. LRRK2 phosphorylation of auxilin mediates synaptic defects in
864 dopaminergic neurons from patients with Parkinson's disease. Proc Natl Acad Sci U S
865 A. 2018;115(21):5576–81. DOI: 10.1073/pnas.1717590115.

866 26. Thomas RS, Henson A, Gerrish A, Jones L, Williams J, Kidd EJ. Decreasing the
867 expression of PICALM reduces endocytosis and the activity of β-secretase:
868 Implications for Alzheimer's disease. BMC Neurosci. 2016;17(1):50. DOI:
869 10.1186/s12868-016-0288-1.

870 27. Soutar AK, Naoumova RP. Autosomal recessive hypercholesterolemia. Semin Vasc
871 Med. 2004;4(3):241–8. DOI: 10.1055/s-2004-861491.

872 28. Maldonado-Báez L, Wendland B. Endocytic adaptors: recruiters, coordinators and
873 regulators [Internet]. Vol. 16, Trends in Cell Biology. 2006. p. 505–13. DOI:
874 10.1016/j.tcb.2006.08.001.

875 29. Henne WM, Boucrot E, Meinecke M, Evergren E, Vallis Y, Mittal R, McMahon HT.
876 FCHo proteins are nucleators of Clathrin-Mediated endocytosis. Science (80- ).
877 2010;328(5983):1281–4. DOI: 10.1126/science.1188462.

878 30. Boucrot E, Pick A, Çamdere G, Liska N, Evergren E, McMahon HT, Kozlov MM.
879 Membrane Fission Is Promoted by Insertion of Amphipathic Helices and Is Restricted

880 by Crescent BAR Domains. Cell. 2012;149(1):124–36. DOI: 10.1016/j.cell.2012.01.047.

881 31. Dannhauser PN, Ungewickell EJ. Reconstitution of clathrin-coated bud and vesicle
882 formation with minimal components. Nat Cell Biol. 2012;14(6):634–9. DOI:
883 10.1038/ncb2478.

884 32. Stabley DR, Jurchenko C, Marshall SS, Salaita KS. Visualizing mechanical tension across
885 membrane receptors with a fluorescent sensor. Nat Methods. 2012;9(1):64–7. DOI:
886 10.1038/nmeth.1747.

887 33. Haucke V, Kozlov MM. Membrane remodeling in clathrin-mediated endocytosis. J Cell
888 Sci. 2018;131(17):jcs216812. DOI: 10.1242/jcs.216812.

889 34. Lacy MM, Ma R, Ravindra NG, Berro J. Molecular mechanisms of force production in
890 clathrin-mediated endocytosis [Internet]. Vol. 592, FEBS Letters. John Wiley & Sons,
891 Ltd; 2018. p. 3586–605. DOI: 10.1002/1873-3468.13192.

892 35. Kirchhausen T, Harrison SC. Protein organization in clathrin trimers. Cell.
893 1981;23(3):755–61. DOI: 10.1016/0092-8674(81)90439-6.

894 36. Ungewickell E, Branton D. Assembly units of clathrin coats. Nature.
895 1981;289(5796):420–2. DOI: 10.1038/289420a0.

896 37. Fotin A, Cheng Y, Sliz P, Grigorieff N, Harrison SC, Kirchhausen T, Walz T. Molecular
897 model for a complete clathrin lattice from electron cryomicroscopy. Nature.
898 2004;432(7017):573–9. DOI: 10.1038/nature03079.

899 38. Chen CY, Reese ML, Hwang PK, Ota N, Agard D, Brodsky FM. Clathrin light and heavy
900 chain interface: α-helix binding superhelix loops via critical tryptophans. EMBO J.

901 2002;21(22):6072–82. DOI: 10.1093/emboj/cdf594.

902 39. Kirchhausen T, Scarmato P, Harrison SC, Monroe JJ, Chow EP, Mattaliano RJ,
903 Ramachandran KL, Smart JE, Ahn AH, Brosius J. Clathrin light chains LCA and LCB are
904 similar, polymorphic, and share repeated heptad motifs. Science (80- ).
905 1987;236(4799):320–4. DOI: 10.1126/science.3563513.

906 40. Kirchhausen T, Toyoda T. Immunoelectron microscopic evidence for the extended
907 conformation of light chains in clathrin trimers. J Biol Chem. 1993;268(14):10268–73.

908 41. Morris KL, Jones JR, Halebian M, Wu S, Baker M, Armache J-P, Avila Ibarra A, Sessions
909 RB, Cameron AD, Cheng Y, Smith CJ. Cryo-EM of multiple cage architectures reveals a
910 universal mode of clathrin self-assembly. Nat Struct Mol Biol. 2019;26(10):890–8.
911 DOI: 10.1038/s41594-019-0292-0.

912 42. Ybe JA, Brodsky FM, Hofmann K, Lin K, Liu S-H, Chen L, Earnest TN, Fletterick RJ,
913 Hwang PK. Clathrin self-assembly is mediated by a tandemly repeated superhelix.
914 Nature. 1999;399(6734):371–5. DOI: 10.1038/20708.

915 43. Ter Haar E, Musacchio A, Harrison SC, Kirchhausen T. Atomic structure of clathrin: A β
916 propeller terminal domain joins an α zigzag linker. Cell. 1998;95(4):563–73. DOI:
917 10.1016/s0092-8674(00)81623-2.

918 44. Pettersen EF, Goddard TD, Huang CC, Couch GS, Greenblatt DM, Meng EC, Ferrin TE.
919 UCSF Chimera - A visualization system for exploratory research and analysis. J Comput
920 Chem. 2004;25(13):1605–12. DOI: 10.1002/jcc.20084.

921 45. Cheng Y, Boll W, Kirchhausen T, Harrison SC, Walz T. Cryo-electron Tomography of

Clathrin-coated Vesicles: Structural Implications for Coat Assembly. J Mol Biol. 2007;365(3):892–9. DOI: 10.1016/j.jmb.2006.10.036.

46. Heymann JB, Winkler DC, Yim Y-I, Eisenberg E, Greene LE, Steven AC. Clathrin-coated vesicles from brain have small payloads: a cryo-electron tomographic study. J Struct Biol. 2013;184(1):43–51. DOI: 10.1016/j.jsb.2013.05.006.

47. Smith CJ, Grigorieff N, Pearse BMF. Clathrin coats at 21 Å resolution: A cellular assembly designed to recycle multiple membrane receptors. EMBO J. 1998;17(17):4943–53. DOI: 10.1093/emboj/17.17.4943.

48. Paraan M, Mendez J, Sharum S, Kurtin D, He H, Stagg SM. The structures of natively assembled clathrin-coated vesicles. Sci Adv. 2020;6(30):eaba8397. DOI: 10.1126/sciadv.aba8397.

49. Ter Haar E, Harrison SC, Kirchhausen T. Peptide-in-groove interactions link target proteins to the beta -propeller of Peptide-in-groove interactions link target proteins to the ᴺL-propeller of clathrin. Proc Natl Acad Sci U S A. 1999;97(3):1096–100. DOI: 10.1073/pnas.97.3.1096.

50. Shih W, Gallusser A, Kirchhausen T. A clathrin-binding site in the hinge of the β2 chain of mammalian AP-2 complexes. J Biol Chem. 1995;270(52):31083–90. DOI: 10.1074/jbc.270.52.31083.

51. Ramjaun AR, McPherson PS. Multiple Amphiphysin II Splice Variants Display Differential Clathrin Binding: Identification of Two Distinct Clathrin-Binding Sites. J Neurochem. 2002;70(6):2369–76. DOI: 10.1046/j.1471-4159.1998.70062369.x.

943 52. Krupnick JG, Goodman OB, Keen JH, Benovic JL. Arrestin/clathrin interaction.
944 Localization of the clathrin binding domain of nonvisual arrestins to the carboxyl
945 terminus. J Biol Chem. 1997;272(23):15011–6. DOI: 10.1074/jbc.272.23.15011.

946 53. Dell'Angelica EC, Klumperman J, Stoorvogel W, Bonifacino JS. Association of the AP-3
947 adaptor complex with clathrin. Science (80- ). 1998;280(5362):431–4. DOI:
948 10.1126/science.280.5362.431.

949 54. Drake MT, Traub LM. Interaction of Two Structurally Distinct Sequence Types with the
950 Clathrin Terminal Domain β-Propeller. J Biol Chem. 2001;276(31):28700–9. DOI:
951 10.1074/jbc.m104226200.

952 55. Kang DS, Kern RC, Puthenveedu MA, von Zastrow M, Williams JC, Benovic JL.
953 Structure of an arrestin2-clathrin complex reveals a novel clathrin binding domain
954 that modulates receptor trafficking. J Biol Chem. 2009;284(43):29860–72. DOI:
955 10.1074/jbc.m109.023366.

956 56. Miele AE, Watson PJ, Evans PR, Traub LM, Owen DJ. Two distinct interaction motifs in
957 amphiphysin bind two independent sites on the clathrin terminal domain β-propeller.
958 Nat Struct Mol Biol. 2004;11(3):242–8. DOI: 10.1038/nsmb736.

959 57. Willox AK, Sahraoui YME, Royle SJ. Non-specificity of Pitstop 2 in clathrin-mediated
960 endocytosis. Biol Open. 2014;3(5):326–31. DOI: 10.1242/bio.20147955.

961 58. Muenzner J, Traub LM, Kelly BT, Graham SC. Cellular and viral peptides bind multiple
962 sites on the N-terminal domain of clathrin. Traffic. 2017;18(1):44–57. DOI:
963 10.1111/tra.12457.

964 59. Zhuo Y, Cano KE, Wang L, Ilangovan U, Hinck AP, Sousa R, Lafer EM. Nuclear magnetic
965 resonance structural mapping reveals promiscuous interactions between clathrin-box
966 motif sequences and the N-terminal domain of the clathrin heavy chain.
967 Biochemistry. 2015;54(16):2571–80. DOI: 10.1021/acs.biochem.5b00065.

968 60. Smith CJ, Dafforn TR, Kent H, Sims CA, Khubchandani-Aswani K, Zhang L, Saibil HR,
969 Pearse BMF. Location of Auxilin Within a Clathrin Cage. J Mol Biol. 2004;336(2):461–
970 71. DOI: 10.1016/j.jmb.2003.12.006.

971 61. Zhuo Y, Ilangovan U, Schirf V, Demeler B, Sousa R, Hinck AP, Lafer EM. Dynamic
972 Interactions between Clathrin and Locally Structured Elements in a Disordered
973 Protein Mediate Clathrin Lattice Assembly. J Mol Biol. 2010;404(2):274–90. DOI:
974 10.1016/j.jmb.2010.09.044.

975 62. Schlosshauer M, Baker D. Realistic protein-protein association rates from a simple
976 diffusional model neglecting long-range interactions, free energy barriers, and
977 landscape ruggedness. Protein Sci. 2004;13(6):1660–9. DOI: 10.1110/ps.03517304.

978 63. Mettlen M, Chen P-H, Srinivasan S, Danuser G, Schmid SL. Regulation of Clathrin-
979 Mediated Endocytosis. Annu Rev Biochem. 2018;87(1):871–96. DOI:
980 10.1146/annurev-biochem-062917-012644.

981 64. Traub LM. Regarding the amazing choreography of clathrin coats. PLoS Biol.
982 2011;9(3):e1001037. DOI: 10.1371/journal.pbio.1001037.

983 65. Merrifield CJ, Feldman ME, Wan L, Almers W. Imaging actin and dynamin recruitment
984 during invagination of single clathrin-coated pits. Nat Cell Biol. 2002;4(9):691–8. DOI:

985 10.1038/ncb837.

986 66. Taylor MJ, Perrais D, Merrifield CJ. A high precision survey of the molecular dynamics
987 of mammalian clathrin-mediated endocytosis. Schmid SL, editor. PLoS Biol.
988 2011;9(3):e1000604. DOI: 10.1371/journal.pbio.1000604.

989 67. Tonikian R, Xin X, Toret CP, Gfeller D, Landgraf C, Panni S, et al. Bayesian modeling of
990 the yeast SH3 domain interactome predicts spatiotemporal dynamics of endocytosis
991 proteins. Walhout M, editor. PLoS Biol. 2009;7(10):e1000218. DOI:
992 10.1371/journal.pbio.1000218.

993 68. Kadlecova Z, Spielman SJ, Loerke D, Mohanakrishnan A, Reed DK, Schmid SL.
994 Regulation of clathrin-mediated endocytosis by hierarchical allosteric activation of
995 AP2. J Cell Biol. 2017;216(1):167–79. DOI: 10.1083/jcb.201608071.

996 69. Umasankar PK, Sanker S, Thieman JR, Chakraborty S, Wendland B, Tsang M, Traub
997 LM. Distinct and separable activities of the endocytic clathrin-coat components
998 Fcho1/2 and AP-2 in developmental patterning. Nat Cell Biol. 2012;14(5):488–501.
999 DOI: 10.1038/ncb2473.

1000 70. Cocucci E, Aguet F, Boulant S, Kirchhausen T. The first five seconds in the life of a
1001 clathrin-coated pit. Cell. 2012;150(3):495–507. DOI: 10.1016/j.cell.2012.05.047.

1002 71. Ma L, Umasankar PK, Wrobel AG, Lymar A, McCoy AJ, Holkar SS, Jha A, Pradhan-
1003 Sundd T, Watkins SC, Owen DJ, Traub LM. Transient Fcho1/2·Eps15/R·AP-2
1004 Nanoclusters Prime the AP-2 Clathrin Adaptor for Cargo Binding. Dev Cell.
1005 2015;37(5):428–43. DOI: 10.1016/j.devcel.2016.05.003.

1006 72. Stimpson HEM, Toret CP, Cheng AT, Pauly BS, Drubin DG. Early-arriving Syp1p and
1007 Ede1p function in endocytic site placement and formation in budding yeast. Schmid
1008 SL, editor. Mol Biol Cell. 2009;20(22):4640–51. DOI: 10.1091/mbc.e09-05-0429.

1009 73. Brach T, Godlee C, Moeller-Hansen I, Boeke D, Kaksonen M. The initiation of clathrin-
1010 mediated endocytosis is mechanistically highly flexible. Curr Biol. 2014;24(5):548–54.
1011 DOI: 10.1016/j.cub.2014.01.048.

1012 74. Brown MS, Goldstein JL. Receptor-mediated endocytosis: insights from the
1013 lipoprotein receptor system. Proc Natl Acad Sci. 1979;76(7):3330–7. DOI:
1014 10.1073/pnas.76.7.3330.

1015 75. Twyman RM. Clathrin and Clathrin-Adaptors. Encycl Neurosci. 2009;1013–7. DOI:
1016 10.1016/b978-008045046-9.01364-4.

1017 76. Ehrlich M, Boll W, Van Oijen A, Hariharan R, Chandran K, Nibert ML, Kirchhausen T.
1018 Endocytosis by random initiation and stabilization of clathrin-coated pits. Cell.
1019 2004;118(5):591–605. DOI: 10.1016/j.cell.2004.08.017.

1020 77. Owen DJ, Collins BM, Evans PR. ADAPTORS FOR CLATHRIN COATS: Structure and
1021 Function. Annu Rev Cell Dev Biol. 2004;20(1):153–91. DOI:
1022 10.1146/annurev.cellbio.20.010403.104543.

1023 78. Traub LM. Tickets to ride: Selecting cargo for clathrin-regulated internalization
1024 [Internet]. Vol. 10, Nature Reviews Molecular Cell Biology. Nature Publishing Group;
1025 2009. p. 583–96. DOI: 10.1038/nrm2751.

1026 79. Koo SJ, Markovic S, Puchkov D, Mahrenholz CC, Beceren-Braun F, Maritzen T,

1027 Dernedde J, Volkmer R, Oschkinat H, Haucke V. SNARE motif-mediated sorting of
1028 synaptobrevin by the endocytic adaptors clathrin assembly lymphoid myeloid
1029 leukemia (CALM) and AP180 at synapses. Proc Natl Acad Sci U S A.
1030 2011;108(33):13540–5. DOI: 10.1073/pnas.1107067108.

1031 80. Liu AP, Aguet F, Danuser G, Schmid SL. Local clustering of transferrin receptors
1032 promotes clathrin-coated pit initiation. J Cell Biol. 2010;191(7):1381–93. DOI:
1033 10.1083/jcb.201008117.

1034 81. Kibbey RG, Rizo J, Gierasch LM, Anderson RG. The LDL receptor clustering motif
1035 interacts with the clathrin terminal domain in a reverse turn conformation. J Cell Biol.
1036 1998;142(1):59–67. DOI: 10.1083/jcb.142.1.59.

1037 82. Henry AG, Hislop JN, Grove J, Thorn K, Marsh M, von Zastrow M. Regulation of
1038 Endocytic Clathrin Dynamics by Cargo Ubiquitination. Dev Cell. 2012;23(3):519–32.
1039 DOI: 10.1016/j.devcel.2012.08.003.

1040 83. Merrifield CJ, Perrais D, Zenisek D. Coupling between clathrin-coated-pit invagination,
1041 cortactin recruitment, and membrane scission observed in live cells. Cell.
1042 2005;121(4):593–606. DOI: 10.1016/j.cell.2005.03.015.

1043 84. Nunez D, Antonescu C, Mettlen M, Liu A, Schmid SL, Loerke D, Danuser G. Hotspots
1044 Organize Clathrin-Mediated Endocytosis by Efficient Recruitment and Retention of
1045 Nucleating Resources. Traffic. 2011;12(12):1868–78. DOI: 10.1111/j.1600-
1046 0854.2011.01273.x.

1047 85. Antonescu CN, Aguet F, Danuser G, Schmid SL. Phosphatidylinositol-(4,5)-

1048 bisphosphate regulates clathrin-coated pit initiation, stabilization, and size.
1049 Gruenberg JE, editor. Mol Biol Cell. 2011;22(14):2588–600. DOI: 10.1091/mbc.e11-
1050 04-0362.

1051 86. Zoncu R, Perera RM, Sebastian R, Nakatsu F, Chen H, Balla T, Ayala G, Toomre D, De
1052 Camilli P V. Loss of endocytic clathrin-coated pits upon acute depletion of
1053 phosphatidylinositol 4,5-bisphosphate. Proc Natl Acad Sci U S A. 2007;104(10):3793–
1054 8. DOI: 10.1073/pnas.0611733104.

1055 87. Carroll SY, Stimpson HEM, Weinberg J, Toret CP, Sun Y, Drubin DG. Analysis of yeast
1056 endocytic site formation and maturation through a regulatory transition point.
1057 Schmid SL, editor. Mol Biol Cell. 2012;23(4):657–68. DOI: 10.1091/mbc.e11-02-0108.

1058 88. Mettlen M, Stoeber M, Loerke D, Antonescu CN, Danuser G, Schmid SL. Endocytic
1059 accessory proteins are functionally distinguished by their differential effects on the
1060 maturation of clathrin-coated pits. Lemmon S, editor. Mol Biol Cell.
1061 2009;20(14):3251–60. DOI: 10.1091/mbc.e09-03-0256.

1062 89. Loerke D, Mettlen M, Yarar D, Jaqaman K, Jaqaman H, Danuser G, Schmid SL. Cargo
1063 and dynamin regulate clathrin-coated pit maturation. Hughson F, editor. PLoS Biol.
1064 2009;7(3):0628–39. DOI: 10. 1371/journal.pbio.1000057.

1065 90. Ford MGJ, Mills IG, Peter BJ, Vallis Y, Praefcke GJK, Evans PR, McMahon HT. Curvature
1066 of clathrin-coated pits driven by epsin. Nature. 2002;419(6905):361–6. DOI:
1067 10.1038/nature01020.

1068 91. Saleem M, Morlot S, Hohendahl A, Manzi J, Lenz M, Roux A. A balance between

1069 membrane elasticity and polymerization energy sets the shape of spherical clathrin
1070 coats. Nat Commun. 2015;6(6249). DOI: 10.1038/ncomms7249.

1071 92. Dannhauser PN, Platen M, Böning H, Ungewickell H, Schaap IAT, Ungewickell EJ.
1072 Effect of Clathrin Light Chains on the Stiffness of Clathrin Lattices and Membrane
1073 Budding. Traffic. 2015;16(5):519–33. DOI: 10.1111/tra.12263.

1074 93. Redlingshöfer L, McLeod F, Chen Y, Camus MD, Burden JJ, Palomer E, Briant K,
1075 Dannhauser PN, Salinas PC, Brodsky FM. Clathrin light chain diversity regulates
1076 membrane deformation in vitro and synaptic vesicle formation in vivo. Proc Natl Acad
1077 Sci. 2020;117(38):23527–38. DOI: 10.1073/pnas.2003662117.

1078 94. Massol RH, Boll W, Griffin AM, Kirchhausen T. A burst of auxilin recruitment
1079 determines the onset of clathrin-coated vesicle uncoating. Proc Natl Acad Sci U S A.
1080 2006;103(27):10265–70. DOI: 10.1073/pnas.0603369103.

1081 95. Schlossman DM, Schmid SL, Braell WA, Rothman JE. An enzyme that removes clathrin
1082 coats: Purification of an uncoating ATPase. J Cell Biol. 1984;99(2):723–33. DOI:
1083 10.1083/jcb.99.2.723.

1084 96. Wu X, Zhao X, Baylor L, Kaushal S, Eisenberg E, Greene LE. Clathrin exchange during
1085 clathrin-mediated endocytosis. J Cell Biol. 2001;155(2):291–300. DOI:
1086 10.1083/jcb.200104085.

1087 97. Loerke D, Wienisch M, Kochubey O, Klingauf J. Differential control of clathrin subunit
1088 dynamics measured with EW-FRAP microscopy. Traffic. 2005;6(10):918–29. DOI:
1089 10.1111/j.1600-0854.2005.00329.x.

1090 98. Avinoam O, Schorb M, Beese CJ, Briggs JAG, Kaksonen M. Endocytic sites mature by
1091 continuous bending and remodeling of the clathrin coat. Science (80- ).
1092 2015;348(6241):1369–72. DOI: 10.1126/science.aaa9555.

1093 99. Sousa R, Liao HS, Cuéllar J, Jin S, Valpuesta JM, Jin AJ, Lafer EM. Clathrin-coat
1094 disassembly illuminates the mechanisms of Hsp70 force generation. Nat Struct Mol
1095 Biol. 2016;23(9):821–9. DOI: 10.1038/nsmb.3272.

1096 100. Picco A, Mund M, Ries J, Nédélec F, Kaksonen M. Visualizing the functional
1097 architecture of the endocytic machinery. Elife. 2015;4:e04535. DOI:
1098 10.7554/elife.04535.

1099 101. Collins A, Warrington A, Taylor KA, Svitkina T. Structural organization of the actin
1100 cytoskeleton at sites of clathrin-mediated endocytosis. Curr Biol. 2011;21(14):1167–
1101 75. DOI: 10.1016/j.cub.2011.05.048.

1102 102. Carlsson AE, Bayly P V. Force generation by endocytic actin patches in budding yeast.
1103 Biophys J. 2014;106(8):1596–606. DOI: 10.1016/j.bpj.2014.02.035.

1104 103. Dmitrieff S, Nédélec F. Membrane Mechanics of Endocytosis in Cells with Turgor.
1105 Ewers H, editor. PLoS Comput Biol. 2015;11(10):e1004538. DOI:
1106 10.1371/journal.pcbi.1004538.

1107 104. Ayscough KR, Stryker J, Pokala N, Sanders M, Crews P, Drubin DG. High rates of actin
1108 filament turnover in budding yeast and roles for actin in establishment and
1109 maintenance of cell polarity revealed using the actin inhibitor latrunculin-A. J Cell
1110 Biol. 1997;137(2):399–416. DOI: 10.1083/jcb.137.2.399.

1111 105. Fujimoto LM, Roth R, Heuser JE, Schmid SL. Actin Assembly Plays a Variable, but not
1112 Obligatory Role in Receptor-Mediated Endocytosis. Traffic. 2000;1(2):161–71. DOI:
1113 10.1034/j.1600-0854.2000.010208.x.

1114 106. Lamaze C, Fujimoto LM, Yin HL, Schmid SL. The actin cytoskeleton is required for
1115 receptor-mediated endocytosis in mammalian cells. J Biol Chem.
1116 1997;272(33):20332–5. DOI: 10.1074/jbc.272.33.20332.

1117 107. Grassart A, Cheng AT, Hong SH, Zhang F, Zenzer N, Feng Y, Briner DM, Davis GD,
1118 Malkov D, Drubin DG. Actin and dynamin2 dynamics and interplay during clathrin-
1119 mediated endocytosis. J Cell Biol. 2014;205(5):721–35. DOI: 10.1083/jcb.201403041.

1120 108. Li D, Shao L, Chen B-C, Zhang X, Zhang M, Moses B, Milkie DE, Beach JR, Hammer JA,
1121 Pasham M, Kirchhausen T, Baird MA, Davidson MW, Xu P, Betzig E. Extended-
1122 resolution structured illumination imaging of endocytic and cytoskeletal dynamics.
1123 Science. 2015;349(6251):aab3500. DOI: 10.1126/science.aab3500.

1124 109. Akamatsu M, Vasan R, Serwas D, Ferrin MA, Rangamani P, Drubin DG. Principles of
1125 self-organization and load adaptation by the actin cytoskeleton during clathrin-
1126 mediated endocytosis. Elife. 2020;9. DOI: 10.7554/elife.49840.

1127 110. Leyton-Puig D, Isogai T, Argenzio E, van den Broek B, Klarenbeek J, Janssen H, Jalink K,
1128 Innocenti M. Flat clathrin lattices are dynamic actin-controlled hubs for clathrin-
1129 mediated endocytosis and signalling of specific receptors. Nat Commun.
1130 2017;8(1):16068. DOI: 10.1038/ncomms16068.

1131 111. Boulant S, Kural C, Zeeh JC, Ubelmann F, Kirchhausen T. Actin dynamics counteract

1132 membrane tension during clathrin-mediated endocytosis. Nat Cell Biol.
1133 2011;13(9):1124–32. DOI: 10.1038/ncb2307.

1134 112. Engqvist-Goldstein ÅEY, Zhang CX, Carreno S, Barroso C, Heuser JE, Drubin DG. RNAi-
1135 mediated Hip1R Silencing Results in Stable Association between the Endocytic
1136 Machinery and the Actin Assembly Machinery. Mol Biol Cell. 2004;15(4):1666–79.
1137 DOI: 10.1091/mbc.e03-09-0639.

1138 113. Messa M, Fernández-Busnadiego R, Sun EW, Chen H, Czapla H, Wrasman K, Wu Y, Ko
1139 G, Ross T, Wendland B, De Camilli P. Epsin deficiency impairs endocytosis by stalling
1140 the actin-dependent invagination of endocytic clathrin-coated pits. Elife.
1141 2014;3:e03311. DOI: 10.7554/elife.03311.

1142 114. Skruzny M, Brach T, Ciuffa R, Rybina S, Wachsmuth M, Kaksonen M. Molecular basis
1143 for coupling the plasma membrane to the actin cytoskeleton during clathrin-
1144 mediated endocytosis. Proc Natl Acad Sci U S A. 2012;109(38):E2533-42. DOI:
1145 10.1073/pnas.1207011109.

1146 115. Skruzny M, Desfosses A, Prinz S, Dodonova SO, Gieras A, Uetrecht C, Jakobi AJ, Abella
1147 M, Hagen WJH, Schulz J, Meijers R, Rybin V, Briggs JAG, Sachse C, Kaksonen M. An
1148 Organized Co-assembly of Clathrin Adaptors Is Essential for Endocytosis. Dev Cell.
1149 2015;33(2):150–62. DOI: 10.1016/j.devcel.2015.02.023.

1150 116. Frost A, Perera R, Roux A, Spasov K, Destaing O, Egelman EH, De Camilli P, Unger VM.
1151 Structural Basis of Membrane Invagination by F-BAR Domains. Cell. 2008;132(5):807–
1152 17. DOI: 10.1016/j.cell.2007.12.041.

1153 117. Habermann B. The BAR-domain family of proteins: A case of bending and binding?
1154 EMBO Rep. 2004;5(3):250–5. DOI: 10.1038/sj.embor.7400105.

1155 118. Mim C, Cui H, Gawronski-Salerno JA, Frost A, Lyman E, Voth GA, Unger VM. Structural
1156 basis of membrane bending by the N-BAR protein endophilin. Cell. 2012;149(1):137–
1157 45. DOI: 10.1016/j.cell.2012.01.048.

1158 119. Schöneberg J, Lehmann M, Ullrich A, Posor Y, Lo WT, Lichtner G, Schmoranzer J,
1159 Haucke V, Noé F. Lipid-mediated PX-BAR domain recruitment couples local
1160 membrane constriction to endocytic vesicle fission. Nat Commun. 2017;8(1):15873.
1161 DOI: 10.1038/ncomms15873.

1162 120. Wu M, Huang B, Graham M, Raimondi A, Heuser JE, Zhuang X, De Camilli P. Coupling
1163 between clathrin-dependent endocytic budding and F-BAR-dependent tubulation in a
1164 cell-free system. Nat Cell Biol. 2010;12(9):902–8. DOI: 10.1038/ncb2094.

1165 121. Itoh T, Erdmann KS, Roux A, Habermann B, Werner H, De Camilli P. Dynamin and the
1166 actin cytoskeleton cooperatively regulate plasma membrane invagination by BAR and
1167 F-BAR proteins. Dev Cell. 2005;9(6):791–804. DOI: 10.1016/j.devcel.2005.11.005.

1168 122. Meinecke M, Boucrot E, Camdere G, Hon W-C, Mittal R, McMahon HT. Cooperative
1169 recruitment of dynamin and BIN/amphiphysin/Rvs (BAR) domain-containing proteins
1170 leads to GTP-dependent membrane scission. J Biol Chem. 2013;288(9):6651–61. DOI:
1171 10.1074/jbc.m112.444869.

1172 123. Antonny B, Burd C, De Camilli P, Chen E, Daumke O, Faelber K, et al. Membrane
1173 fission by dynamin: what we know and what we need to know. EMBO J.

1174 2016;35(21):2270–84. DOI: 10.15252/embj.201694613.

1175 124. Morlot S, Roux A. Mechanics of dynamin-mediated membrane fission. Annu Rev
1176 Biophys. 2013;42:629–49. DOI: 10.1146/annurev-biophys-050511-102247.

1177 125. Ingerman E, Perkins EM, Marino M, Mears JA, McCaffery JM, Hinshaw JE, Nunnari J.
1178 Dnm1 forms spirals that are structurally tailored to fit mitochondria. J Cell Biol.
1179 2005;170(7):1021–7. DOI: 10.1083/jcb.200506078.

1180 126. Miserey-Lenkei S, Chalancon G, Bardin S, Formstecher E, Goud B, Echard A. Rab and
1181 actomyosin-dependent fission of transport vesicles at the Golgi complex. Nat Cell
1182 Biol. 2010;12(7):645–54. DOI: 10.1038/ncb2067.

1183 127. Slepnev VI, De Camilli P. Accessory factors in clathrin-dependent synaptic vesicle
1184 endocytosis. Nat Rev Neurosci. 2000;1(3):161–72. DOI: 10.1038/35044540.

1185 128. Watanabe S, Mamer LE, Raychaudhuri S, Luvsanjav D, Eisen J, Trimbuch T, Söhl-
1186 Kielczynski B, Fenske P, Milosevic I, Rosenmund C, Jorgensen EM. Synaptojanin and
1187 Endophilin Mediate Neck Formation during Ultrafast Endocytosis. Neuron.
1188 2018;98(6):1184-1197.e6. DOI: 10.1016/j.neuron.2018.06.005.

1189 129. McPherson PS, Garcia EP, Slepnev VI, David C, Zhang X, Grabs D, Sossin WS,
1190 Bauerfeind R, Nemoto Y, De Camilli P. A presynaptic inositol-5-phosphatase. Nature.
1191 1996;379(6563):353–7. DOI: 10.1038/379353a0.

1192 130. Cremona O, Di Paolo G, Wenk MR, Lüthi A, Kim WT, Takei K, Daniell L, Nemoto Y,
1193 Shears SB, Flavell RA, McCormick DA, De Camilli P. Essential role of phosphoinositide
1194 metabolism in synaptic vesicle recycling. Cell. 1999;99(2):179–88. DOI:

1195 10.1016/s0092-8674(00)81649-9.

1196 131. Nández R, Balkin DM, Messa M, Liang L, Paradise S, Czapla H, Hein MY, Duncan JS,
1197 Mann M, De Camilli P. A role of OCRL in clathrin-coated pit dynamics and uncoating
1198 revealed by studies of Lowe syndrome cells. Elife. 2014;3:e02975. DOI:
1199 10.7554/elife.02975.

1200 132. He K, Song E, Upadhyayula S, Dang S, Gaudin R, Skillern W, Bu K, Capraro BR,
1201 Rapoport I, Kusters I, Ma M, Kirchhausen T. Dynamics of Auxilin 1 and GAK in clathrin-
1202 mediated traffic. J Cell Biol. 2020;219(3). DOI: 10.1083/jcb.201908142.

1203 133. He K, Marsland III R, Upadhyayula S, Song E, Dang S, Capraro BR, Wang W, Skillern W,
1204 Gaudin R, Ma M, Kirchhausen T. Dynamics of phosphoinositide conversion in clathrin-
1205 mediated endocytic traffic. Nature. 2017;552(7685):410–4. DOI:
1206 10.1038/nature25146.

1207 134. Chang-Ileto B, Frere SG, Chan RB, Voronov S V, Roux A, Di Paolo G. Synaptojanin 1-
1208 mediated PI(4,5)P2 hydrolysis is modulated by membrane curvature and facilitates
1209 membrane fission. Dev Cell. 2011;20(2):206–18. DOI: 10.1016/j.devcel.2010.12.008.

1210 135. Di Paolo G, De Camilli P. Phosphoinositides in cell regulation and membrane
1211 dynamics. Nature. 2006;443(7112):651–7. DOI: 10.1038/nature05185.

1212 136. Traub LM. Common principles in clathrin-mediated sorting at the Golgi and the
1213 plasma membrane. Biochim Biophys Acta - Mol Cell Res. 2005;1744(3):415–37. DOI:
1214 10.1016/j.bbamcr.2005.04.005.

1215 137. Ahle S, Ungewickell E. Auxilin, a newly identified clathrin-associated protein in coated

1216 vesicles from bovine brain. J Cell Biol. 1990;111(1):19–29. DOI: 10.1083/jcb.111.1.19.

1217 138. Schroder S, Morris SA, Knorr R, Plessmann U, Weber K, Vinh NG, Ungewickell E.
1218 Primary Structure of the Neuronal Clathrin-Associated Protein Auxilin and its
1219 Expression in Bacteria. Eur J Biochem. 1995;228(2):297–304. DOI: 10.1111/j.1432-
1220 1033.1995.0297n.x.

1221 139. Ungewickell E, Ungewickell H, Holstein SEH, Lindner R, Prasad K, Barouch W, Martini
1222 B, Greene LE, Eisenberg E. Role of auxilin in uncoating clathrin-coated vesicles.
1223 Nature. 1995;378(6557):632–5. DOI: 10.1038/378632a0.

1224 140. Holstein SE, Ungewickell H, Ungewickell E. Mechanism of clathrin basket dissociation:
1225 separate functions of protein domains of the DnaJ homologue auxilin. J Cell Biol.
1226 1996;135(4):925–37. DOI: 10.1083/jcb.135.4.925.

1227 141. Fotin A, Cheng Y, Grigorieff N, Walz T, Harrison SC, Kirchhausen T. Structure of an
1228 auxilin-bound clathrin coat and its implications for the mechanism of uncoating.
1229 Nature. 2004;432(7017):649–53. DOI: 10.1038/nature03078.

1230 142. Braell WA, Schlossman DM, Schmid SL, Rothman JE. Dissociation of clathrin coats
1231 coupled to the hydrolysis of ATP: Role of an uncoating ATPase. J Cell Biol.
1232 1984;99(2):735–41. DOI: 10.1083/jcb.99.2.734.

1233 143. Kalli AC, Morgan G, Sansom MSP. Interactions of the Auxilin-1 PTEN-like Domain with
1234 Model Membranes Result in Nanoclustering of Phosphatidyl Inositol Phosphates.
1235 Biophys J. 2013;105(1):137–45. DOI: 10.1016/j.bpj.2013.05.012.

1236 144. Park B-C, Yim Y-I, Zhao X, Olszewski MB, Eisenberg E, Greene LE. The clathrin-binding

1237 and J-domains of GAK support the uncoating and chaperoning of clathrin by Hsc70 in
1238 the brain. J Cell Sci. 2015;128(20):3811–21. DOI: 10.1242/jcs.171058.

1239 145. Ungewickell E, Ungewickell H, Holstein SE. Functional interaction of the auxilin J
1240 domain with the nucleotide- and substrate-binding modules of Hsc70. J Biol Chem.
1241 1997;272(31):19594–600. DOI: 10.1074/jbc.272.31.19594.

1242 146. Barouch W, Prasad K, Greene L, Eisenberg E. Auxilin-Induced Interaction of the
1243 Molecular Chaperone Hsc70 with Clathrin Baskets. Biochemistry. 1997;36(14):4303–
1244 8. DOI: 10.1021/bi962727z.

1245 147. Young A, Stoilova-McPhie S, Rothnie A, Vallis Y, Harvey-Smith P, Ranson N, Kent H,
1246 Brodsky FM, Pearse BMF, Roseman A, Smith CJ. Hsc70-induced Changes in Clathrin-
1247 Auxilin Cage Structure Suggest a Role for Clathrin Light Chains in Cage Disassembly.
1248 Traffic. 2013;14(9):987–96. DOI: 10.1111/tra.12085.

1249 148. Barouch W, Prasad K, Greene LE, Eisenberg E. ATPase activity associated with the
1250 uncoating of clathrin baskets by Hsp70. J Biol Chem. 1994;269(46):28563–8.

1251 149. Prasad K, Barouch W, Greene L, Eisenberg E. A protein cofactor is required for
1252 uncoating of clathrin baskets by uncoating ATPase. J Biol Chem. 1993;268(32):23758–
1253 61. DOI: 10.1016/s0021-9258(20)80445-1.

1254 150. Greene MK, Maskos K, Landry SJ. Role of the J-domain in the cooperation of Hsp40
1255 with Hsp70. Proc Natl Acad Sci. 1998;95(11):6108–13. DOI: 10.1073/pnas.95.11.6108.

1256 151. Xue Y-L, Zhou L, Sun Y, Li H, Jones GW, Song Y. Steered molecular dynamics
1257 simulation of the binding of the bovine auxilin J domain to the Hsc70 nucleotide-

1258 binding domain. J Mol Model. 2017;23(320). DOI: 10.1007/s00894-017-3453-2.

1259 152. Rapoport I, Boll W, Yu A, Böcking T, Kirchhausen T. A Motif in the Clathrin Heavy
1260 Chain Required for the Hsc70/Auxilin Uncoating Reaction. Mol Biol Cell.
1261 2008;19(1):405–13. DOI: 10.1091/mbc.e07-09-0870.

1262 153. Xing Y, Böcking T, Wolf M, Grigorieff N, Kirchhausen T, Harrison SC. Structure of
1263 clathrin coat with bound Hsc70 and auxilin: mechanism of Hsc70-facilitated
1264 disassembly. EMBO J. 2010;29(3):655–65. DOI: 10.1038/emboj.2009.383.

1265 154. Sousa R, Lafer EM. The role of molecular chaperones in clathrin mediated vesicular
1266 trafficking. Front Mol Biosci. 2015;2(26). DOI: 10.3389/fmolb.2015.00026.

1267 155. Böcking T, Aguet F, Rapoport I, Banzhaf M, Yu A, Zeeh JC, Kirchhausen T. Key
1268 Interactions for Clathrin Coat Stability. Structure. 2014;22(6):819–29. DOI:
1269 10.1016/j.str.2014.04.002.

1270 156. Sousa R. Structural mechanisms of chaperone mediated protein disaggregation. Front
1271 Mol Biosci. 2014;1(12). DOI: 10.3389/fmolb.2014.00012.

1272 157. Böcking T, Aguet F, Harrison SC, Kirchhausen T. Single-molecule analysis of a
1273 molecular disassemblase reveals the mechanism of Hsc70-driven clathrin uncoating.
1274 Nat Struct Mol Biol. 2011;18(3):295–301. DOI: 10.1038/nsmb.1985.

1275 158. Ferreira F, Foley M, Cooke A, Cunningham M, Smith G, Woolley R, Henderson G, Kelly
1276 E, Mundell S, Smythe E. Endocytosis of G Protein-Coupled Receptors Is Regulated by
1277 Clathrin Light Chain Phosphorylation. Curr Biol. 2012;22(15):1361–70. DOI:
1278 10.1016/j.cub.2012.05.034.

1279 159. Krantz KC, Puchalla J, Thapa R, Kobayashi C, Bisher M, Viehweg J, Carr CM, Rye HS.
1280 Clathrin Coat Disassembly by the Yeast Hsc70/Ssa1p and Auxilin/Swa2p Proteins
1281 Observed by Single-particle Burst Analysis Spectroscopy. J Biol Chem.
1282 2013;288(37):26721. DOI: 10.1074/jbc.m113.491753.

1283 160. Rothnie A, Clarke AR, Kuzmic P, Cameron A, Smith CJ. A sequential mechanism for
1284 clathrin cage disassembly by 70-kDa heat-shock cognate protein (Hsc70) and auxilin.
1285 Proc Natl Acad Sci U S A. 2011;108(17):6927–32. DOI: 10.1073/pnas.1018845108.

1286 161. Packschies L, Theyssen H, Buchberger A, Bukau B, Goody R, Reinstein J. GrpE
1287 accelerates nucleotide exchange of the molecular chaperone DnaK with an
1288 associative displacement mechanism. Biochemistry. 1997;36(12):3417–22. DOI:
1289 10.1021/bi962835l.

1290 162. McCarty JS, Buchberger A, Reinstein J, Bukau B. The Role of ATP in the Functional
1291 Cycle of the DnaK Chaperone System. J Mol Biol. 1995;249(1):126–37. DOI:
1292 10.1006/jmbi.1995.0284.

1293 163. Takeda S, McKay DB. Kinetics of Peptide Binding to the Bovine 70 kDa Heat Shock
1294 Cognate Protein, a Molecular Chaperone [†]. Biochemistry. 1996;35(14):4636–44. DOI:
1295 10.1021/bi952903o.

1296 164. Theyssen H, Schuster H-P, Packschies L, Bukau B, Reinstein J. The Second Step of ATP
1297 Binding to DnaK Induces Peptide Release. J Mol Biol. 1996;263(5):657–70. DOI:
1298 10.1006/jmbi.1996.0606.

1299 165. Morgan JR, Jiang J, Oliphint PA, Jin S, Gimenez LE, Busch DJ, Foldes AE, Zhuo Y, Sousa

1300 R, Lafer EM. A Role for an Hsp70 Nucleotide Exchange Factor in the Regulation of
1301 Synaptic Vesicle Endocytosis. J Neurosci. 2013;33(18):8009. DOI:
1302 10.1523/jneurosci.4505-12.2013.

1303 166. Lee D-W, Wu X, Eisenberg E, Greene LE. Recruitment dynamics of GAK and auxilin to
1304 clathrin-coated pits during endocytosis. J Cell Sci. 2006;119(Pt 17):3502–12. DOI:
1305 10.1242/jcs.03092.

1306 167. Sousa R, Lafer EM. The Physics of Entropic Pulling: A Novel Model for the Hsp70
1307 Motor Mechanism. Int J Mol Sci. 2019;20(9). DOI: 10.3390/ijms20092334.

1308 168. Goloubinoff P, Rios PDL. The mechanism of Hsp70 chaperones: (entropic) pulling the
1309 models together. Trends Biochem Sci. 2007;32(8):372–80. DOI:
1310 10.1016/j.tibs.2007.06.008.

1311 169. Rios PDL, Ben-Zvi A, Slutsky O, Azem A, Goloubinoff P. Hsp70 chaperones accelerate
1312 protein translocation and the unfolding of stable protein aggregates by entropic
1313 pulling. Proc Natl Acad Sci. 2006;103(16):6166–71. DOI: 10.1073/pnas.0510496103.

1314 170. Kirchhausen T. Clathrin. Annu Rev Biochem. 2000;69(1):699–727. DOI:
1315 10.1146/annurev.biochem.69.1.699.

1316 171. Ramanan V, Agrawal NJ, Liu J, Engles S, Toy R, Radhakrishnan R. Systems biology and
1317 physical biology of clathrin-mediated endocytosis. Integr Biol (Camb). 2011;3(8):803–
1318 15. DOI: 10.1039/c1ib00036e.

1319 172. Akisaka T, Yoshida A. Surface distribution of heterogenous clathrin assemblies in
1320 resorbing osteoclasts. Exp Cell Res. 2021;399(1):112433. DOI:

1321 10.1016/j.yexcr.2020.112433.

1322 173. Royle SJ. The role of clathrin in mitotic spindle organisation. J Cell Sci. 2012;125:19–
1323 28. DOI: 10.1242/jcs.094607.

1324 174. Hepler PK, McIntosh JR, Cleland S. INTERMICROTUBULE BRIDGES IN MITOTIC SPINDLE
1325 APPARATUS. J Cell Biol. 1970;45(2):438–44. DOI: 10.1083/jcb.45.2.438.

1326 175. Elkhatib N, Bresteau E, Baschieri F, Rioja AL, van Niel G, Vassilopoulos S, Montagnac
1327 G. Tubular clathrin/AP-2 lattices pinch collagen fibers to support 3D cell migration.
1328 Science. 2017;356(6343). DOI: 10.1126/science.aal4713.

1329 176. Milosevic I. Revisiting the Role of Clathrin-Mediated Endoytosis in Synaptic Vesicle
1330 Recycling. Front Cell Neurosci. 2018;12:27. DOI: 10.3389/fncel.2018.00027.

1331 177. Casamento A, Boucrot E. Molecular mechanism of Fast Endophilin-Mediated
1332 Endocytosis. Biochem J. 2020;477(12):2327–45. DOI: 10.1042/bcj20190342.

1333 178. Milosevic I, Giovedi S, Lou X, Raimondi A, Collesi C, Shen H, Paradise S, O'Toole E,
1334 Ferguson S, Cremona O, De Camilli P. Recruitment of endophilin to clathrin-coated pit
1335 necks is required for efficient vesicle uncoating after fission. Neuron. 2011;72(4):587–
1336 601. DOI: 10.1016/j.neuron.2011.08.029.

1337 179. Bertot L, Grassart A, Lagache T, Nardi G, Basquin C, Olivo-Marin J-C, Sauvonnet N.
1338 Quantitative and Statistical Study of the Dynamics of Clathrin-Dependent and -
1339 Independent Endocytosis Reveal a Differential Role of EndophilinA2. Cell Rep.
1340 2018;22(6):1574–88. DOI: 10.1016/j.celrep.2018.01.039.

1341 180. Chanaday NL, Cousin MA, Milosevic I, Watanabe S, Morgan JR. The Synaptic Vesicle

1342 Cycle Revisited: New Insights into the Modes and Mechanisms. J Neurosci.
1343 2019;39(42):8209–16. DOI: 10.1523/jneurosci.1158-19.2019.

1344 181. Murdoch JD, Rostosky CM, Gowrisankaran S, Arora AS, Soukup S-F, Vidal R, Capece V,
1345 Freytag S, Fischer A, Verstreken P, Bonn S, Raimundo N, Milosevic I. Endophilin-A
1346 Deficiency Induces the Foxo3a-Fbxo32 Network in the Brain and Causes Dysregulation
1347 of Autophagy and the Ubiquitin-Proteasome System. Cell Rep. 2016;17(4):1071–86.
1348 DOI: 10.1016/j.celrep.2016.09.058.

1349 182. Kasprowicz J, Kuenen S, Miskiewicz K, Habets RLP, Smitz L, Verstreken P. Inactivation
1350 of clathrin heavy chain inhibits synaptic recycling but allows bulk membrane uptake. J
1351 Cell Biol. 2008;182(5):1007–16. DOI: 10.1083/jcb.200804162.

1352 183. Augustine GJ, Morgan JR, Villalba-Galea CA, Jin S, Prasad K, Lafer EM. Clathrin and
1353 synaptic vesicle endocytosis: studies at the squid giant synapse. Biochem Soc Trans.
1354 2006;34(1):68–72. DOI: 10.1042/bst0340068.

1355 184. Farsi Z, Gowrisankaran S, Krunic M, Rammner B, Woehler A, Lafer EM, Mim C, Jahn R,
1356 Milosevic I. Clathrin coat controls synaptic vesicle acidification by blocking vacuolar
1357 ATPase activity. Elife. 2018;7. DOI: 10.7554/elife.32569.

1358 185. Calebiro D, Godbole A. Internalization of G-protein-coupled receptors: Implication in
1359 receptor function, physiology and diseases. Best Pract Res Clin Endocrinol Metab.
1360 2018;32(2):83–91. DOI: 10.1016/j.beem.2018.01.004.

1361 186. Ferrandon S, Feinstein TN, Castro M, Wang B, Bouley R, Potts JT, Gardella TJ,
1362 Vilardaga J-P. Sustained cyclic AMP production by parathyroid hormone receptor

1363 endocytosis. Nat Chem Biol. 2009;5(10):734–42. DOI: 10.1038/nchembio.206.

1364 187. Tsao PI, von Zastrow M. Type-specific sorting of G protein-coupled receptors after
1365 endocytosis. J Biol Chem. 2000;275(15):11130–40. DOI: 10.1074/jbc.275.15.11130.

1366 188. Ferguson SS. Evolving concepts in G protein-coupled receptor endocytosis: the role in
1367 receptor desensitization and signaling. Pharmacol Rev. 2001;53(1):1–24.

1368 189. Zhang X, Kim K-M. Multifactorial Regulation of G Protein-Coupled Receptor
1369 Endocytosis. Biomol Ther (Seoul). 2017;25(1):26–43. DOI:
1370 10.4062/biomolther.2016.186.

1371 190. Oakley RH, Laporte SA, Holt JA, Barak LS, Caron MG. Association of beta-arrestin with
1372 G protein-coupled receptors during clathrin-mediated endocytosis dictates the profile
1373 of receptor resensitization. J Biol Chem. 1999;274(45):32248–57. DOI:
1374 10.1074/jbc.274.45.32248.

1375 191. Laporte SA, Oakley RH, Holt JA, Barak LS, Caron MG. The interaction of beta-arrestin
1376 with the AP-2 adaptor is required for the clustering of beta 2-adrenergic receptor into
1377 clathrin-coated pits. J Biol Chem. 2000;275(30):23120–6. DOI:
1378 10.1074/jbc.m002581200.

1379 192. Goodman OB, Krupnick JG, Santini F, Gurevich V V., Penn RB, Gagnon AW, Keen JH,
1380 Benovic JL. β-Arrestin acts as a clathrin adaptor in endocytosis of the β2-adrenergic
1381 receptor. Nature. 1996;383(6599):447–50. DOI: 10.1038/383447a0.

1382 193. McArdle CA, Franklin J, Green L, Hislop JN. Signalling, cycling and desensitisation of
1383 gonadotrophin-releasing hormone receptors. J Endocrinol. 2002;173(1):1–11. DOI:

1384 10.1677/joe.0.1730001.

1385 194. Krupnick JG, Benovic JL. The role of receptor kinases and arrestins in G protein-
1386 coupled receptor regulation. Annu Rev Pharmacol Toxicol. 1998;38:289–319. DOI:
1387 10.1146/annurev.pharmtox.38.1.289.

1388 195. Eichel K, von Zastrow M. Subcellular Organization of GPCR Signaling. Trends
1389 Pharmacol Sci. 2018;39(2):200–8. DOI: 10.1016/j.tips.2017.11.009.

1390 196. Qiao Y, Yang J., Zhang X., Liu Y, Zhang J., Zong S., Miao S., Wang L., Koide S.
1391 Characterization of rtSH3p13 gene encoding a development protein involved in
1392 vesicular traffic in spermiogenesis. Cell Res. 2004;14(3):197–207.

1393 197. WEI-PANG H, HAN-CHEN H. Role of microtubule-dependent membrane trafficking in
1394 acrosomal biogenesis. Cell Tissue Res. 2006;323(3):495–503.

1395 198. Funaki T, Kon S, Tanabe K, Natsume W, Sato S, Shimizu T, et al. The Arf GAP SMAP2 is
1396 necessary for organized vesicle budding from the trans-Golgi network and
1397 subsequent acrosome formation in spermiogenesis. Mol Biol Cell. 2013;24(17):2633–
1398 44. DOI: 10.1091/mbc.e13-05-0234.

1399 199. Li S, Qiao Y, Di Q, Le X, Zhang L, Zhang X, Zhang C, Cheng J, Zong S, Koide SS, Miao S,
1400 Wang L. Interaction of SH3P13 and DYDC1 protein: a germ cell component that
1401 regulates acrosome biogenesis during spermiogenesis. Eur J Cell Biol. 2009;88:509–
1402 20. DOI: 10.1016/j.ejcb.2009.05.001.

1403 200. Ezratty EJ, Bertaux C, Marcantonio EE, Gundersen GG. Clathrin mediates integrin
1404 endocytosis for focal adhesion disassembly in migrating cells. J Cell Biol.

1405 2009;187(5):733–47. DOI: 10.1083/jcb.200904054.

1406 201. Chao W-T, Kunz J. Focal adhesion disassembly requires clathrin-dependent
1407 endocytosis of integrins. FEBS Lett. 2009;583(8):1337–43. DOI:
1408 10.1016/j.febslet.2009.03.037.

1409 202. Geraldo S, Simon A, Elkhatib N, Louvard D, Fetler L, Vignjevic DM. Do cancer cells
1410 have distinct adhesions in 3D collagen matrices and in vivo? Eur J Cell Biol.
1411 2012;91(11–12):930–7. DOI: 10.1016/j.ejcb.2012.07.005.

1412 203. Tawil N, Wilson P, Carbonetto S. Integrins in point contacts mediate cell spreading:
1413 factors that regulate integrin accumulation in point contacts vs. focal contacts. J Cell
1414 Biol. 1993;120(1):261–71. DOI: 10.1083/jcb.120.1.261.

1415 204. Maupin P, Pollard TD. Improved preservation and staining of HeLa cell actin filaments,
1416 clathrin-coated membranes, and other cytoplasmic structures by tannic acid-
1417 glutaraldehyde-saponin fixation. J Cell Biol. 1983;96(1):51–62. DOI:
1418 10.1083/jcb.96.1.51.

1419 205. Borlido J, Veltri G, Jackson AP, Mills IG. Clathrin Is Spindle-Associated but Not
1420 Essential for Mitosis. Keen J, editor. PLoS One. 2008;3(9):e3115. DOI:
1421 10.1371/journal.pone.0003115.

1422 206. Fielding AB, Willox AK, Okeke E, Royle SJ. Clathrin-mediated endocytosis is inhibited
1423 during mitosis. Proc Natl Acad Sci U S A. 2012;109(17):6572–7. DOI:
1424 10.1073/pnas.1117401109.

1425 207. Booth DG, Hood FE, Prior IA, Royle SJ. A TACC3/ch-TOG/clathrin complex stabilises

1426 kinetochore fibres by inter-microtubule bridging. EMBO J. 2011;30(5):906–19. DOI:
1427 10.1038/emboj.2011.15.

1428 208. Medendorp K, Vreede L, van Groningen JJM, Hetterschijt L, Brugmans L, Jansen PAM,
1429 van den Hurk WH, de Bruijn DRH, van Kessel AG. The Mitotic Arrest Deficient Protein
1430 MAD2B Interacts with the Clathrin Light Chain A during Mitosis. Ling P, editor. PLoS
1431 One. 2010;5(11):e15128. DOI: 10.1371/journal.pone.0015128.

1432 209. Royle SJ, Lagnado L. Trimerisation is important for the function of clathrin at the
1433 mitotic spindle. J Cell Sci. 2006;119(Pt 19):4071–8. DOI: 10.1242/jcs.03192.

1434 210. Hood FE, Williams SJ, Burgess SG, Richards MW, Roth D, Straube A, Pfuhl M, Bayliss R,
1435 Royle SJ. Coordination of adjacent domains mediates TACC3–ch-TOG–clathrin
1436 assembly and mitotic spindle binding. J Cell Biol. 2013;202(3):463–78. DOI:
1437 10.1083/jcb.201211127.

1438 211. Lin C-H, Hu C-K, Shih H-M. Clathrin heavy chain mediates TACC3 targeting to mitotic
1439 spindles to ensure spindle stability. J Cell Biol. 2010;189(7):1097–105. DOI:
1440 10.1083/jcb.200911120.

1441 212. Rondelet A, Lin Y-C, Singh D, Porfetye AT, Thakur HC, Hecker A, Brinkert P, Schmidt N,
1442 Bendre S, Müller F, Mazul L, Widlund PO, Bange T, Hiller M, Vetter IR, Bird AW.
1443 Clathrin's adaptor interaction sites are repurposed to stabilize microtubules during
1444 mitosis. J Cell Biol. 2020;219(2). DOI: 10.1083/jcb.201907083.

1445 213. Nixon FM, Gutiérrez-Caballero C, Hood FE, Booth DG, Prior IA, Royle SJ. The mesh is a
1446 network of microtubule connectors that stabilizes individual kinetochore fibers of the

1447 mitotic spindle. Elife. 2015;4. DOI: 10.7554/elife.07635.

1448 214. Dickson RB, Willingham MC, Pastan I. alpha 2-macroglobulin adsorbed to colloidal
1449 gold: a new probe in the study of receptor-mediated endocytosis. J Cell Biol.
1450 1981;89(1):29–34. DOI: 10.1083/jcb.89.1.29.

1451 215. Dahlberg JE. Quantitative electron microscopic analysis of the penetration of VSV into
1452 L cells. Virology. 1974;58(1):250–62. DOI: 10.1016/0042-6822(74)90159-7.

1453 216. Fan DP, Sefton BM. The entry into host cells of Sindbis virus, vesicular stomatitis virus
1454 and Sendai virus. Cell. 1978;15(3):985–92. DOI: 10.1016/0092-8674(78)90282-9.

1455 217. Matlin KS, Reggio H, Helenius A, Simons K. Pathway of vesicular stomatitis virus entry
1456 leading to infection. J Mol Biol. 1982;156(3):609–31. DOI: 10.1016/0022-
1457 2836(82)90269-8.

1458 218. Mercer J, Schelhaas M, Helenius A. Virus Entry by Endocytosis. Annu Rev Biochem.
1459 2010;79(1):803–33. DOI: 10.1146/annurev-biochem-060208-104626.

1460 219. Veiga E, Cossart P. Listeria hijacks the clathrin-dependent endocytic machinery to
1461 invade mammalian cells. Nat Cell Biol. 2005;7(9):894–900. DOI: 10.1038/ncb1292.

1462 220. Veiga E, Guttman JA, Bonazzi M, Boucrot E, Toledo-Arana A, Lin AE, Enninga J, Pizarro-
1463 Cerdá J, Finlay BB, Kirchhausen T, Cossart P. Invasive and adherent bacterial
1464 pathogens co-Opt host clathrin for infection. Cell Host Microbe. 2007;2(5):340–51.
1465 DOI: 10.1016/j.chom.2007.10.001.

1466 221. Bonazzi M, Vasudevan L, Mallet A, Sachse M, Sartori A, Prevost M-C, Roberts A, Taner
1467 SB, Wilbur JD, Brodsky FM, Cossart P. Clathrin phosphorylation is required for actin

1468 recruitment at sites of bacterial adhesion and internalization. J Cell Biol.
1469 2011;195(3):525–36. DOI: 10.1083/jcb.201105152.

1470 222. Pizarro-Cerdá J, Kühbacher A, Cossart P. Entry of Listeria monocytogenes in
1471 mammalian epithelial cells: an updated view. Cold Spring Harb Perspect Med.
1472 2012;2(11). DOI: 10.1101/cshperspect.a010009.

1473 223. Veiga E, Cossart P. The role of clathrin-dependent endocytosis in bacterial
1474 internalization. Trends Cell Biol. 2006;16(10):499–504. DOI:
1475 10.1016/j.tcb.2006.08.005.

1476 224. Moreno-Ruiz E, Galán-Díez M, Zhu W, Fernández-Ruiz E, d'Enfert C, Filler SG, Cossart
1477 P, Veiga E. Candida albicans internalization by host cells is mediated by a clathrin-
1478 dependent mechanism. Cell Microbiol. 2009;11(8):1179–89. DOI: 10.1111/j.1462-
1479 5822.2009.01319.x.

1480 225. Almeida RA, Oliver SP. Invasion of Bovine Mammary Epithelial Cells by Streptococcus
1481 dysgalactiae. J Dairy Sci. 1995;78(6):1310–7. DOI: 10.3168/jds.s0022-0302(95)76752-
1482 2.

1483 226. Jevon M, Guo C, Ma B, Mordan N, Nair SP, Harris M, Henderson B, Bentley G, Meghji
1484 S. Mechanisms of internalization of Staphylococcus aureus by cultured human
1485 osteoblasts. Infect Immun. 1999;67(5):2677–81. DOI: 10.1128/iai.67.5.2677-
1486 2681.1999.

1487 227. Fumagalli M, Camus SM, Diekmann Y, Burke A, Camus MD, Norman PJ, Joseph A, Abi-
1488 Rached L, Benazzo A, Rasteiro R, Mathieson I, Topf M, Parham P, Thomas MG,

1489 Brodsky FM. Genetic diversity of CHC22 clathrin impacts its function in glucose
1490 metabolism. Elife. 2019;8. DOI: 10.7554/elife.41517.

1491 228. Wakeham DE, Abi-Rached L, Towler MC, Wilbur JD, Parham P, Brodsky FM. Clathrin
1492 heavy and light chain isoforms originated by independent mechanisms of gene
1493 duplication during chordate evolution. Proc Natl Acad Sci U S A. 2005;102(20):7209–
1494 14. DOI: 10.1073/pnas.0502058102.

1495 229. Hoshino S, Sakamoto K, Vassilopoulos S, Camus SM, Griffin CA, Esk C, Torres JA,
1496 Ohkoshi N, Ishii A, Tamaoka A, Funke BH, Kucherlapati R, Margeta M, Rando TA,
1497 Brodsky FM. The CHC22 Clathrin-GLUT4 Transport Pathway Contributes to Skeletal
1498 Muscle Regeneration. Rappoport JZ, editor. PLoS One. 2013;8(10):e77787. DOI:
1499 10.1371/journal.pone.0077787.

1500 230. Gould GW, Brodsky FM, Bryant NJ. Building GLUT4 Vesicles: CHC22 Clathrin's Human
1501 Touch. Trends Cell Biol. 2020;30(9):705–19. DOI: 10.1016/j.tcb.2020.05.007.

1502 231. Camus SM, Camus MD, Figueras-Novoa C, Boncompain G, Sadacca LA, Esk C, Bigot A,
1503 Gould GW, Kioumourtzoglou D, Perez F, Bryant NJ, Mukherjee S, Brodsky FM. CHC22
1504 clathrin mediates traffic from early secretory compartments for human GLUT4
1505 pathway biogenesis. J Cell Biol. 2020;219(1). DOI: 10.1083/jcb.201812135.

1506 232. Dannhauser PN, Camus SM, Sakamoto K, Sadacca LA, Torres JA, Camus MD, Briant K,
1507 Vassilopoulos S, Rothnie A, Smith CJ, Brodsky FM. CHC22 and CHC17 clathrins have
1508 distinct biochemical properties and display differential regulation and function. J Biol
1509 Chem. 2017;292(51):20834–44. DOI: 10.1074/jbc.m117.816256.

1510 233. Nossal R. Energetics of clathrin basket assembly. Traffic. 2001;2(2):138–47. DOI:
1511 10.1034/j.1600-0854.2001.020208.x.

1512 234. Jin AJ, Nossal R. Rigidity of triskelion arms and clathrin nets. Biophys J.
1513 2000;78(3):1183–94. DOI: 10.1016/s0006-3495(00)76676-8.

1514 235. Chen Z, Schmid SL. Evolving models for assembling and shaping clathrin-coated pits. J
1515 Cell Biol. 2020;219(9). DOI: 10.1083/jcb.202005126.

1516 236. Kirchhausen T. Coated pits and coated vesicles - sorting it all out. Curr Opin Struct
1517 Biol. 1993;3(2):182–8. DOI: 10.1016/s0959-440x(05)80150-2.

1518 237. Jin AJ, Nossal R. Topological mechanisms involved in the formation of clathrin-coated
1519 vesicles. Biophys J. 1993;65(4):1523–37. DOI: 10.1016/s0006-3495(93)81189-5.

1520 238. Heuser J, Evans L. Three-dimensional visualization of coated vesicle formation in
1521 fibroblasts. J Cell Biol. 1980;84(3):560–83. DOI: 10.1083/jcb.84.3.560.

1522 239. Grove J, Metcalf DJ, Knight AE, Wavre-Shapton ST, Sun T, Protonotarios ED, Griffin LD,
1523 Lippincott-Schwartz J, Marsh M. Flat clathrin lattices: stable features of the plasma
1524 membrane. Mol Biol Cell. 2014;25(22):3581–94. DOI: 10.1091/mbc.e14-06-1154.

1525 240. Subtil A, Gaidarov I, Kobylarz K, Lampson MA, Keen JH, McGraw TE. Acute cholesterol
1526 depletion inhibits clathrin-coated pit budding. Proc Natl Acad Sci U S A.
1527 1999;96(12):6775–80. DOI: 10.1073/pnas.96.12.6775.

1528 241. Chen Y, Yong J, Martínez-Sánchez A, Yang Y, Wu Y, De Camilli P, Fernández-
1529 Busnadiego R, Wu M. Dynamic instability of clathrin assembly provides proofreading
1530 control for endocytosis. J Cell Biol. 2019;218(10):3200–11. DOI:

1531 10.1083/jcb.201804136.

1532 242. Hirst J, Sahlender DA, Li S, Lubben NB, Borner GHH, Robinson MS. Auxilin Depletion
1533 Causes Self-Assembly of Clathrin into Membraneless Cages *In Vivo*. Traffic.
1534 2008;9(8):1354–71. DOI: 10.1111/j.1600-0854.2008.00764.x.

1535 243. Yim Y-I, Scarselletta S, Zang F, Wu X, Lee D, Kang Y, Eisenberg E, Greene LE. Exchange
1536 of clathrin, AP2 and epsin on clathrin-coated pits in permeabilized tissue culture cells.
1537 J Cell Sci. 2005;117(4):631–9. DOI: 10.1242/jcs.00910.

1538 244. Bucher D, Frey F, Sochacki KA, Kummer S, Bergeest J-P, Godinez WJ, Kräusslich H-G,
1539 Rohr K, Taraska JW, Schwarz US, Boulant S. Clathrin-adaptor ratio and membrane
1540 tension regulate the flat-to-curved transition of the clathrin coat during endocytosis.
1541 Nat Commun. 2018;9(1109). DOI: 10.1038/s41467-018-03533-0.

1542 245. Sochacki KA, Heine BL, Haber GJ, Jimah JR, Prasai B, Alfonzo-Mendez MA, Roberts AD,
1543 Somasundaram A, Hinshaw JE, Taraska JW. The structure and spontaneous curvature
1544 of clathrin lattices at the plasma membrane. bioRxiv. 2020;2020.07.18.207258. DOI:
1545 10.1101/2020.07.18.207258.

1546 246. Ferguson JP, Willy NM, Heidotting SP, Huber SD, Webber MJ, Kural C. Deciphering
1547 dynamics of clathrin-mediated endocytosis in a living organism. J Cell Biol.
1548 2016;214(3):347–58. DOI: 10.1083/jcb.201604128.

1549 247. Willy NM, Ferguson JP, Silahli S, Cakez C, Hasan F, Chen Y, Wu M, Chang HC, Travesset
1550 A, Li S, Zandi R, Li D, Betzig E, Cocucci E, Kural C. Endocytic Clathrin Coats Develop
1551 Curvature at Early Stages of Their Formation. bioRxiv. 2019;(715219). DOI:

1552 10.1101/715219.

1553 248. Scott BL, Sochacki KA, Low-Nam ST, Bailey EM, Luu Q, Hor A, Dickey AM, Smith S,
1554 Kerkvliet JG, Taraska JW, Hoppe AD. Membrane bending occurs at all stages of
1555 clathrin-coat assembly and defines endocytic dynamics. Nat Commun. 2018;9(419).
1556 DOI: 10.1038/s41467-018-02818-8.

1557 249. Maib H, Ferreira F, Vassilopoulos S, Smythe E. Cargo regulates clathrin-coated pit
1558 invagination via clathrin light chain phosphorylation. J Cell Biol. 2018;217(12):4253–
1559 66. DOI: 10.1083/jcb.201805005.

1560 250. Keen JH, Willingham MC, Pastan IH. Clathrin-coated vesicles: isolation, dissociation
1561 and factor-dependent reassociation of clathrin baskets. Cell. 1979;16(2):303–12. DOI:
1562 10.1016/0092-8674(79)90007-2.

1563 251. Schook W, Puszkin S, Bloom W, Ores C, Kochwa S. Mechanochemical properties of
1564 brain clathrin: interactions with actin and alpha-actinin and polymerization into
1565 basketlike structures or filaments. Proc Natl Acad Sci U S A. 1979;76(1):116–20. DOI:
1566 10.1073/pnas.76.1.116.

1567 252. Nandi PK, Pretorius HT, Lippoldt RE, Johnson ML, Edelhoch H. Molecular properties of
1568 the reassembled coat protein of coated vesicles. Biochemistry. 1980;19(25):5917–21.
1569 DOI: 10.1021/bi00566a039.

1570 253. Woodward MP, Roth TF. Coated vesicles: characterization, selective dissociation, and
1571 reassembly. Proc Natl Acad Sci U S A. 1978;75(9):4394–8. DOI:
1572 10.1073/pnas.75.9.4394.

1573 254. Crowther RA, Pinch JT, Pearse BMF. On the structure of coated vesicles. J Mol Biol.
1574 1976;103(4):785–98. DOI: 10.1016/0022-2836(76)90209-6.

1575 255. Sorger PK, Crowther RA, Finch JT, Pearse BM. Clathrin cubes: an extreme variant of
1576 the normal cage. J Cell Biol. 1986;103(4):1213–9. DOI: 10.1083/jcb.103.4.1213.

1577 256. Heuser JE, Keen JH, Amende LM, Lippoldt RE, Prasad K. Deep-etch visualization of 27S
1578 clathrin: a tetrahedral tetramer. J Cell Biol. 1987;105(5):1999–2009. DOI:
1579 10.1083/jcb.105.5.1999.

1580 257. Dannhauser PN, Platen M, Böning H, Schaap IAT. Durable protein lattices of clathrin
1581 that can be functionalized with nanoparticles and active biomolecules. Nat
1582 Nanotechnol. 2015;10(11):954–7. DOI: 10.1038/nnano.2015.206.

1583 258. Ferguson ML, Prasad K, Boukari H, Sackett DL, Krueger S, Lafer EM, Nossal R. Clathrin
1584 triskelia show evidence of molecular flexibility. Biophys J. 2008;95(4):1945–55. DOI:
1585 10.1529/biophysj.107.126342.

1586 259. Ungewickells E, Ungewickell H. Bovine Brain Clathrin Light Chains Impede Heavy
1587 Chain Assembly in Vitro*. J Biol Chem. 1991;266(19):12710–4. DOI: 10.1016/s0021-
1588 9258(18)98957-x.

1589 260. Liu SH, Wong ML, Craik CS, Brodsky FM. Regulation of clathrin assembly and
1590 trimerization defined using recombinant triskelion hubs. Cell. 1995;83(2):257–67.
1591 DOI: 10.1016/0092-8674(95)90167-1.

1592 261. Wilbur JD, Hwang PK, Ybe JA, Lane M, Sellers BD, Jacobson MP, Fletterick RJ, Brodsky
1593 FM. Conformation Switching of Clathrin Light Chain Regulates Clathrin Lattice

1594 Assembly. Dev Cell. 2010;18(5):854–61. DOI: 10.1016/j.devcel.2010.04.007.

1595 262. Ybe JA, Ruppel N, Mishra S, VanHaaften E. Contribution of Cysteines to Clathrin
1596 Trimerization Domain Stability and Mapping of Light Chain Binding. Traffic.
1597 2003;4(12):850–6. DOI: 10.1046/j.1600-0854.2003.0139.x.

1598 263. Ybe JA, Perez-Miller S, Niu Q, Coates DA, Drazer MW, Clegg ME. Light Chain C-
1599 Terminal Region Reinforces the Stability of Clathrin Heavy Chain Trimers. Traffic.
1600 2007;8(8):1101–10. DOI: 10.1111/j.1600-0854.2007.00597.x.

1601 264. Musacchio A, Smith CJ, Roseman AM, Harrison SC, Kirchhausen T, Pearse BM.
1602 Functional organization of clathrin in coats: combining electron cryomicroscopy and
1603 X-ray crystallography. Mol Cell. 1999;3(6):761–70. DOI: 10.1016/s1097-
1604 2765(01)80008-3.

1605 265. Kovtun O, Dickson VK, Kelly BT, Owen DJ, Briggs JAG. Architecture of the AP2/clathrin
1606 coat on the membranes of clathrin-coated vesicles. Sci Adv. 2020;6(30):eaba8381.
1607 DOI: 10.1126/sciadv.aba8381.

1608 266. Bhave M, Mino RE, Wang X, Lee J, Grossman HM, Lakoduk AM, Danuser G, Schmid SL,
1609 Mettlen M. Functional characterization of 67 endocytic accessory proteins using
1610 multiparametric quantitative analysis of CCP dynamics. Proc Natl Acad Sci U S A.
1611 2020;117(50):31591–602. DOI: 10.1073/pnas.2020346117.

1612 267. Dandey VP, Budell WC, Wei H, Bobe D, Maruthi K, Kopylov M, et al. Time-resolved
1613 cryo-EM using Spotiton. Nat Methods. 2020;17(9):897–900. DOI: 10.1038/s41592-
1614 020-0925-6.

1615